Discovery of Clonixeril as a Sub-Femtomolar Modulator of the Human STING Receptor

Robert P. Sparks[1,2,3†], William Lawless[1,2,4†], Anna Kharitonova[1,2,4†], Rainer Metcalf[1†], Jamie Nunziata[1], Grace A. Binder[1], Sauradip Chaudhuri[5], Christine S.R. Gambino[1], Michelle Wilde[1], Linette S. Harding[1], Jaret J. Crews[1], Mansi Gopu[1], Emilia Dalamangas[1], Sarah Lawless[1], Mark Eschenfelder[1], Robert M. Green[5], Elizabeth X Nompleggi[3,7], Timothy Tran[6], Kathy Yang[6], Donna V. Trask[1], Paul R. Thompson[5], Rekha Patel[2,4], Niketa A. Patel[2,4], Wesley H. Brooks[1], W. Guy Bradley[8], Mildred E. Acevedo-Duncan[1], Alan C. Mullen[3], James W. Leahy[1,4,9], Kenyon G. Daniel[1,10], Wayne C. Guida[1,6,9*]

Affiliations:

[1] Department of Chemistry; University of South Florida, Tampa, FL, USA.
[2] Research Service; James A. Haley Veterans Hospital, Tampa, FL, USA.
[3] Division of Gastroenterology, Department of Medicine; University of Massachusetts Chan Medical School, Worcester, Massachusetts, USA.
[4] Department of Molecular Medicine, Morsani College of Medicine; University of South Florida, Tampa, FL, USA.
[5] Biochemistry and Molecular Biotechnology Department; University of Massachusetts Chan Medical School, Worcester, Massachusetts, USA.
[6] H. Lee Moffitt Cancer Center, Research Institute at the University of South Florida; Tampa, FL, USA.
[7] College of the Holy Cross, *Worcester, MA, USA.*
[8] Tampa Bay Research Institute, St. Petersburg, Florida, USA
[9] Florida Center for Drug Discovery and Innovation, University of South Florida, Tampa, FL, USA
[10] Department of Molecular Biosciences, University of South Florida, Tampa, FL, USA.

* Corresponding Author: Dr. Wayne C. Guida, Department of Chemistry, University of South Florida, CHE 205, 4202 E. Fowler Avenue, Tampa, FL 33620, USA

† These authors contributed equally.

Keywords: STING, 2',3'-cGAMP, cyclic-di-GMP, IFN, IRF-3, NSC 335504, Clonixeril, CXL, Clonixin, CXN

Abstract

Stimulator of interferon genes (STING) is a transmembrane endoplasmic reticulum (ER) resident protein involved in innate immunity. STING activation occurs by binding of cyclic guanosine-(2'→5')-monophosphate-adenosine-(3'→5')-monophosphate (2',3'-cGAMP) to STING, which leads to downstream production of type 1 interferons (IFN-1). We generated molecular dynamics (MD) equilibrated agonist and antagonist models of human STING (hSTING) for computer-based screening and now report the discovery of clonixeril (CXL) as the most potent non-nucleotide hSTING modulator discovered to date. We demonstrate *in vitro* and *in cellulo* that CXL has two modes of interaction with hSTING, one with an EC_{50} above 1 nM and the other with an EC_{50} in the 1 fM - 100 aM range (10^{-15}–10^{-16} M). In cell-based experiments, when CXL is titrated below 1 nM, it displays inverse dose dependent antagonistic behavior toward hSTING. We have substantiated that CXL displays this

exceptionally strong inhibitory effect on hSTING mediated IFN-1 production using a THP-1 cell luciferase reporter for interferon regulatory factor 3 (IRF3). Further characterization of CXL was performed in HEK293 cells and by using biophysical and biochemical techniques.

Synopsis

The discovery and properties of clonixeril are described. It was found to have both agonist and antagonist properties relative the STING receptor. It was also found to exhibit unprecedented sub-femtomolar potency as STING antagonist.

Introduction

In mammalian cells, recognition of cytosolic DNA occurs largely through the cyclic GMP-AMP synthase enzyme (cGAS), which functions upstream of the stimulator of interferon genes (STING) protein.[1] Activation of the cGAS-STING pathway results in activation of the innate arm of the immune system.[1] It is cGAS, a surveillance protein, that produces cyclic GMP-AMP (cyclic guanosine-(2'→5')-monophosphate-adenosine-(3'→5')-monophosphate or 2',3'-cGAMP) as the endogenous activator of the STING pathway (see **Figure 1A** for chemical structures).[1-3] cGAS is widely distributed throughout subcellular sites, including the cytosol, the inner leaflet of the plasma membrane, and the nucleus.[2, 3] There are a substantial number of DNA sources that can trigger cGAS enzymatic activity such as from bacteria or a virus.[4] Moreover, mitochondrial dysfunction, augmented rates of cellular apoptosis, and disturbance of phagocytic digestion in combination with DNase deficiencies, like TREX1 mutations can result in cGAS activation.[4]

Figure 1

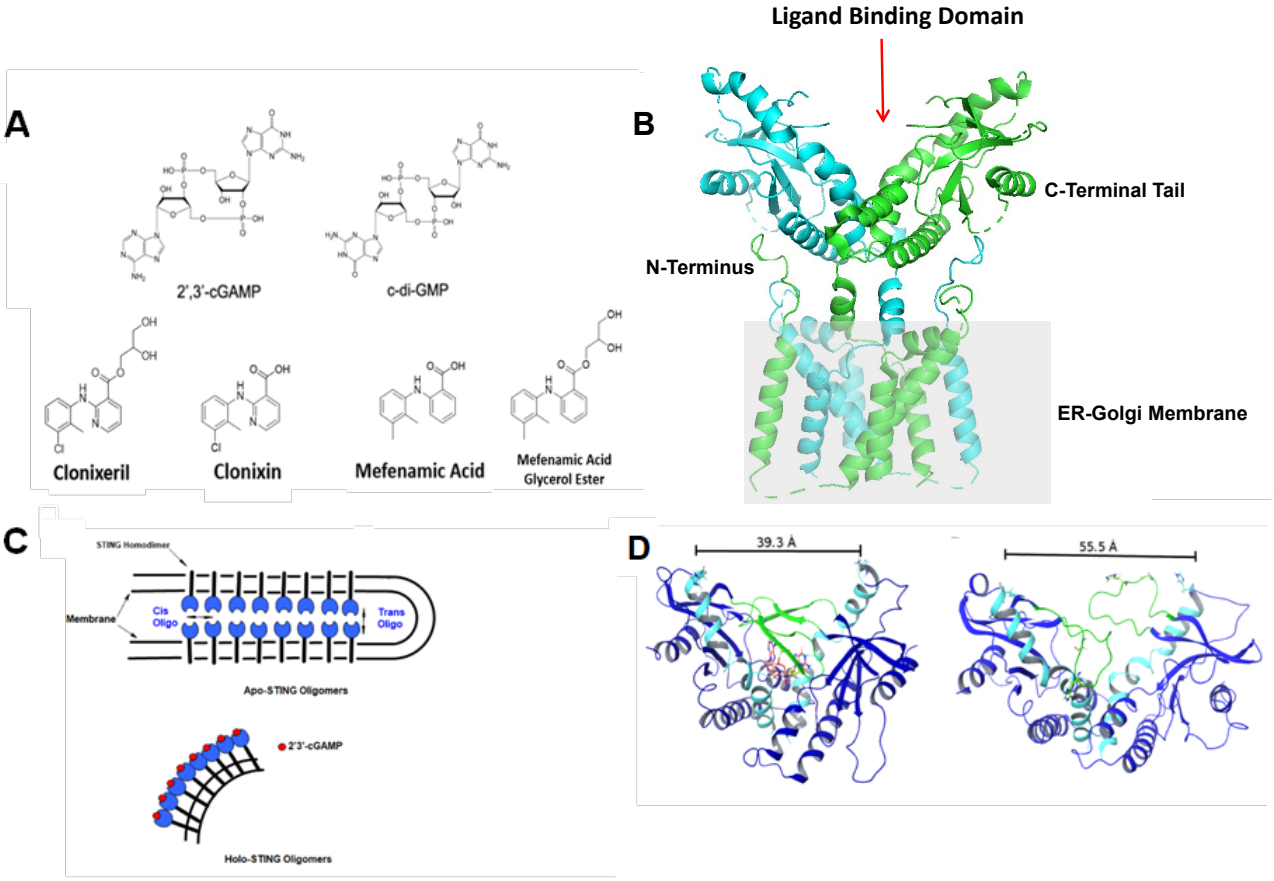

Figure 1. Chemical and Protein Structures. (A) Chemical structures of known STING nucleotide activators plus clonixeril (CXL), clonixin, (CXN) and their analogs, mefenamic acid (MFA), and mefenamic acid glycerol ester (MFE). (B) Cryo-EM structure of full length apo-hSTING (R232). PDB: 6NT5 at a resolution of 4.1 Å. Illustrates the protein ribbon structure with annotations of specific structural components (Left). Overlay the STING protein surface onto the STING ribbon structure (Right). The grey box represents the ER membrane.[5] (C) Model of STING Oligomerization. Depicts two known forms of STING oligomerization, either *cis* or *trans*; generalized after Liu, et al.[6] Apo-STING and Holo-STING are depicted. (D) Distances across nucleotide binding region of STING taken from PDB: 4KSY minimized using Schrödinger software and subjected to MD simulations which indicate a closed (Left) 2',3'-cGAMP bound state (red carbons) and an open apo state (Right) of STING. "Lid" region demarcated with green ribbon and α1 and α2 helix in light blue.[7]

STING is a mediator of innate immunity, including induction of pro-inflammatory cytokine expression, autophagy, and lysosomal cell death.[8, 9] STING is an endoplasmic reticulum (ER) resident protein that is, in its resting state, locally retained within the ER by a Ca^{2+} sensor, stromal interaction molecule 1 (STIM1).[10, 11] Note, though, that this has been challenged on the basis of recent CryoEM studies.[5] STING possesses a transmembrane domain that spans the ER membrane (**Figure 1B**).[5, 11] The carboxy terminal domain (CTD) bears two major amino acid motifs, a highly conserved PLPLRT/SD motif for binding of TANK-binding kinase 1 (TBK1), along with an adjacent pLxIS motif, essential for recruitment and phosphorylation of interferon regulatory factor 3 (IRF3).[12-15] Under steady state conditions, STING forms a domain-swapped homodimer so that its ligand binding domains (LBD's) create a V-shaped site suitable for binding of one cyclic dinucleotide (CDN).[7, 16] In the apo state,

STING is oligomerized within the folds of the ER in a head to head manner (referred to as *trans* oligomers) and lateral side to side (*cis*) oligomers (**Figure 1C**).[6] This zipper-like geometry maintains STING in an autoinhibitory state and ER resident state until activated by 2',3'-cGAMP.[6] Binding of 2',3'-cGAMP induces formation of fully closed dimer angles and the LBD's rotation in relation to the transmembrane domain, bringing about a shift in geometry that permits the STING bilayer to split into bent active STING monolayers to provide highly condensed *cis* oligomers consisting of lateral stacking of the now fully closed STING dimers.[6, 7]

The bent holo structure shown in **Figure 1C**, ultimately forms a vesicle that is transported to the Golgi.[6] Additionally, formation of the protein-ligand complex induces a conformational change involving repositioning of the STING C-terminal tail (CTT).[6] The CTT provides a second autoinhibitory mechanism which results in the protection of the cis oligomer interface, thereby discouraging condensed *cis* oligomerization from prematurely taking place.[6] The condensed *cis* oligomeric structures are stabilized *via* disulfide linkages between vicinal C148 units, which is imperative for STING to gain signaling competence.[6, 17] These oligomers properly position the kinase domains of one TBK1 dimer relative to another TBK1 dimer (located on an adjacent STING dimers) so that trans-phosphorylation of TBK1 can occur.[18] Subsequent phosphorylation occurs when TBK1 exerts its catalytic activity on the S366 residue within the pLxIS motif of the neighboring STING dimer.[13] The endoplasmic-reticulum-Golgi intermediate compartment (ERGIC) serves as an origination site for IRF3 activation.[19] Phosphorylation of STING's pLxIS motif initiates recruitment and binding of IRF3 molecules, positioning them near the active site of TBK1 where phosphorylation of IRF3 occurs.[5, 13, 15] As STING travels through the compartment, the greatest signal transduction is achieved by means of further cluster formation upon arrival of STING at the Golgi.[20] Once phosphorylated, IRF3 undergoes dimerization and subsequent nuclear translocation where it binds to promoter regions to induce type 1 interferon (IFN-1) production.[15] Downregulation of aberrant cGAS-STING activity could alleviate a wide range of inflammatory disorders including the lethal complications that arise from the cytokine storm that can follow SARS-CoV-2 infections.[21-25]

Here, we describe the discovery of clonixeril (CXL) as a potent inhibitor of hSTING, with activity even into attomolar (10^{-18} M) concentrations. Cellular assays using THP-1 and HEK293 cells were performed to assess the effect of CXL on hSTING *in cellulo*. Further characterization of CXL was performed using surface plasmon resonance (SPR), microscale thermophoresis (MST), dynamic light scattering (DLS), and isothermal titration calorimetry (ITC) and native PAGE to study the interaction between CXL and hSTING.

Results

To identify a small molecule that was not a cyclic dinucleotide but could modulate STING activity, we employed computational modeling commencing with molecular dynamics (MD) equilibrated crystal structures for the C-terminal domain (CTD) of human wild-type STING (hSTING^{WT} CTD, **Figure 1D**). Computational models developed for hSTING^{WT} agonists and antagonists informed selection of candidates that were initially screened using a differential scanning fluorescence (thermal shift) assay followed by a THP-1 cell luciferase reporter assay for the pIRF3 dimer binding to its promoter. We identified a low molecular weight compound from the NCI Diversity Set (available from the National Cancer Institute), NSC 335504 (clonixeril, abbrv. CXL), as a potential modulator of hSTING^{WT}. We determined that CXL has weak agonist activity at micromolar concentrations and further found that administration of CXL at low femtomolar (10^{-15} M), and in some cases even attomolar (10^{-18} M) concentrations, resulted in antagonism of the hSTING^{WT} pathway. Notably, clonixin (CXN; **Figure 1A**), which is the carboxylic acid precursor of CXL, exhibited no antagonistic effect. Our data suggest CXL to be the most potent hSTING^{WT} antagonist reported to date with unprecedented potency in the high attomolar range.

Computational Model Construction

In general, wild-type hSTING, C-terminal domain (CTD) structures were employed for computational studies and biophysical studies (subsequently, we refer to this as hSTING CTD). We employed MD simulations to better understand how hSTING CTD interacts with endogenous ligands and other potential binding partners using PDB: 4EMU apo-hSTING and PDB: 4KSY;4F5Y holo-hSTING CTD structures. The distance between the α-carbons of H185A and H185B residues at the end of the α2

helices in dimeric hSTING CTD was used as a metric for full-length hSTING activation. Crystal structures of known agonists exhibited α-carbon distances in the range of 34 to 38 Å for holo structures, whereas apo crystal structures had α-carbon distances in the range of 47 to 56 Å. This prompted the generation of two separate docking models (**Figure 1D**) to screen for (a) agonists, compounds that have greater affinity for the holo (i.e., 2',3'-cGAMP bound structure, PDB: 4KSY) and (b) antagonists, compounds with greater affinity for the apo structure (i.e., c-di-GMP, PDB: 4F5Y). Current docking programs are restricted to docking and evaluating a single molecule at a time. As a result, docking algorithms are unable to effectively handle ligands that bind as dimers, such as the binding of DMXAA to mouse STING.[26] To overcome this limitation, we developed a simple docking method that can be used in conjunction with standard virtual screening protocols to assist in identifying potential small molecule dimer-protein complexes (see Supporting Information).

Computational Docking using hSTING Models

Docking was performed on both MD equilibrated hSTING CTD antagonist and hSTING CTD agonist models (**Figure 1D).** Virtual screening of the NCI Diversity Set was performed using the GLIDE docking program (Schrödinger, Inc.). Also, a ligand-based algorithm (Pharmer) was employed for pharmacophore guided virtual screening of larger compound libraries.[27] The pharmacophore was derived from the X-ray structure of hSTING CTD with 2'3'-cGAMP bound (PDB:4LOH), and the entire ZINC database was screened.[28] Then, ~4000 pharmacophore matched molecules were docked to our hSTING CTD computer models. Next, we examined the top ranking "hits" from virtual screening and subsequently the pharmacophore-based hits *via* a thermal shift assay (**Figure S1**), which led to the discovery of CXL as a possible hSTING binder. The site-restriction docking protocol we developed (see supplementary text) suggests that two CXL molecules bind to the hSTING CTD **(Figure S2D)**.

Clonixeril Demonstrates Unprecedented Potency in the THP-1 Luciferase Reporter Assay

Initially we were encouraged because CXL exhibited agonist activity at micromolar concentrations in THP-1 cells (**Figure 2A**) and, thus, could potentially serve as a lead compound to develop more potent agonists. However, upon further experimentation we were surprised to discover that decreasing CXL to femtomolar concentrations resulted in antagonism of the hSTING pathway

(**Figure 2B**). Accordingly, the WT-THP-1 QUANTI-Luc™ luminescence IRF3 reporter assay was employed in which THP-1 cells were treated with CXL at concentrations ranging from 1 nM – 100 aM for one hour followed by treatment with 4μM 2',3'-cGAMP for an additional 19 hours. The results are shown in (**Figure 2B),** and demonstrate an inverse dose response where lower concentrations of CXL are associated with a decreased response of hSTING to 2',3'-cGAMP activation**.**

To validate our initial observations that CXL has extraordinary potency for a small molecule antagonist, we extended our THP-1 cell luciferase reporter experiment by using diABZI3 as an agonist and using BBCl-amidine (a previously reported STING antagonist) as an antagonist control.[23, 29] Furthermore, because the results were so unprecedented, we conducted these experiments in a different laboratory (U. Mass Chan. vs. Univ. So. FL) and with different individuals performing the experiments. DiABZI3 was used as a STING activator because it is highly potent, it is cell membrane permeable, and it provides an alternative activator to 2,'3'-cGAMP, which is not stable to phosphodiesterases.[23, 30] Thus, Invitrogen's WT-THP-1 QUANTI-Luc™ luminescence assay was performed using 50 nM diABZI3 in the presence of CXL at concentrations ranging from 100 nM to 100 aM. These results confirmed the extraordinary potency of CXL, and the inverse dose response previously observed (**Figure 2 B**). It is noteworthy that as shown in **Figure 2C**, higher concentrations of CXL result in enhancement of the diABZI3 signal.

Figure 2

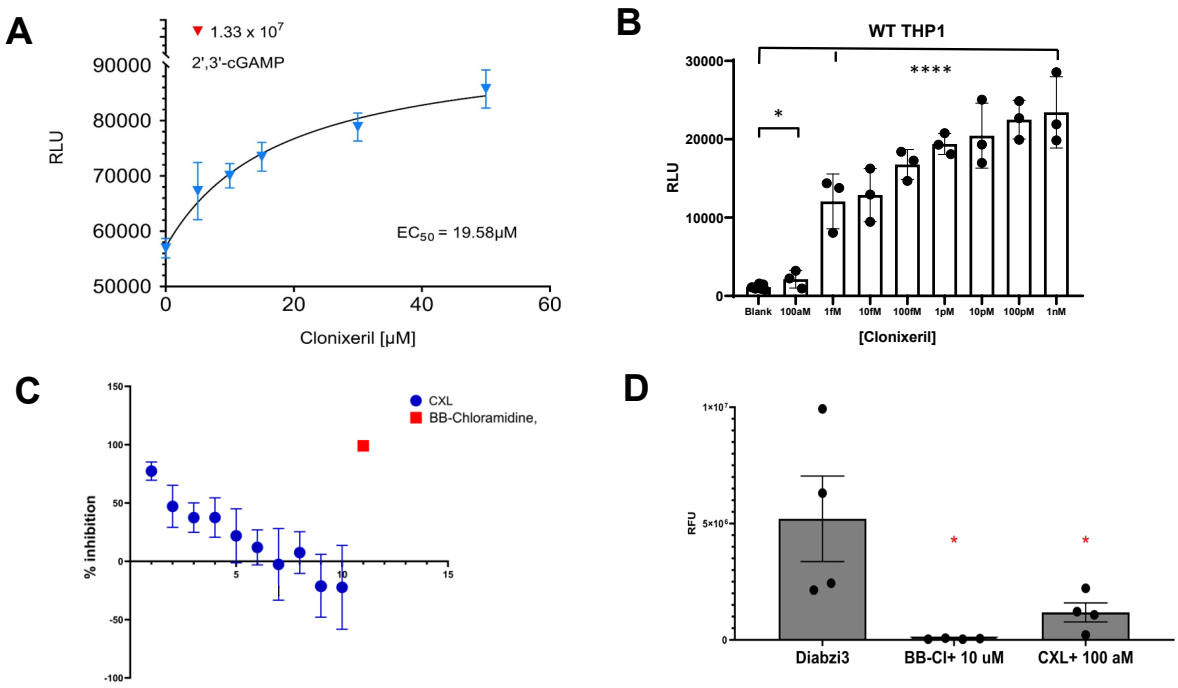

Figure 2. Luciferase assay utilizing monocytic leukemia (THP-1) cells. Cells (Invivogen THP1 Dual™ KI-hSTING-R232; wild type) were analyzed for activation of the hSTING WT pathway *via* an IRF3 luciferase reporter. Luminescence is reported in relative luminescence units (RLU). Error bars are SEM. **A.** Dose-response of THP-1 cells treated with various concentrations of clonixeril (CXL); N=6. The red data point indicates the response of 2',3'-cGAMP positive control at 50μM. **B.** Competition of THP-1 cells treated first with CXL (1hr) and subsequently treated with 2',3'-cGAMP (9hrs); N=3; 2',3'-cGAMP positive control contains 2',3'-cGAMP, 4μM. **C.** Dose-response of THP-1 cells treated with CXL or BB-chloramidine, a known STING antagonist, in the presence of 50 nM diABZI3. Dose range was in 1:10 from 100 aM to 100 nM (1= 100 aM, 2= 1 fM, 3 = 10 fM, 4= 100 fM, 5 = 1 pM, 6 = 10 pM, 7 = 100 pM, 8 = 1 nM, 9= 10 nM, 1 = 100 nM; N=4. Results were plotted in GraphPad Prism. **D.** Quantification of Figure 3C at 100 aM clonixeril and 10 μM BB-chloramidine in the presence of 50 nM diABZI3. *p-value <0.05 via one way ANOVA test generated from GraphPad Prism.

Clonixeril Inhibits 2',3'-cGAMP-Dependent Production of p-hSTING in HEK293 cells

Since phosphorylation of Ser366 of hSTING is a necessary step to initiate recruitment, subsequent docking, and phosphorylation of IRF3, we investigated whether CXL would affect hSTING phosphorylation levels *in cellulo*. Thus, HEK293 cells were treated with varying concentrations of CXL (1fM-1nM) for one hour prior to 2 μM 2',3'-cGAMP treatment for 90 minutes (**Figure 3A**) or 2 hours (**Figure 3C**). An optimized dose of 2 μM 2',3'-cGAMP was based on a dose-response study done for this experiment. A control group was treated with vehicle for 1 hour followed by 2 μM 2',3'-cGAMP for 1 or 2 hours (**Figure 3C**) Total protein lysates were collected and analyzed by Western blotting using antibodies against p-hSTING, hSTING, and β-actin. The Western blot data demonstrated a drastic increase in hSTING phosphorylation levels in the positive control groups. Treatment with varying concentrations of CXL prior to 2',3'-cGAMP downregulated hSTING phosphorylation close to near basal cellular levels (**Figures 3A-C)**. Notably, when HEK293 cells

were treated with 2',3'-cGAMP prior to CXL, inhibitory activity was not observed in the same concentration range (**Figure 3B**).

Figure 3

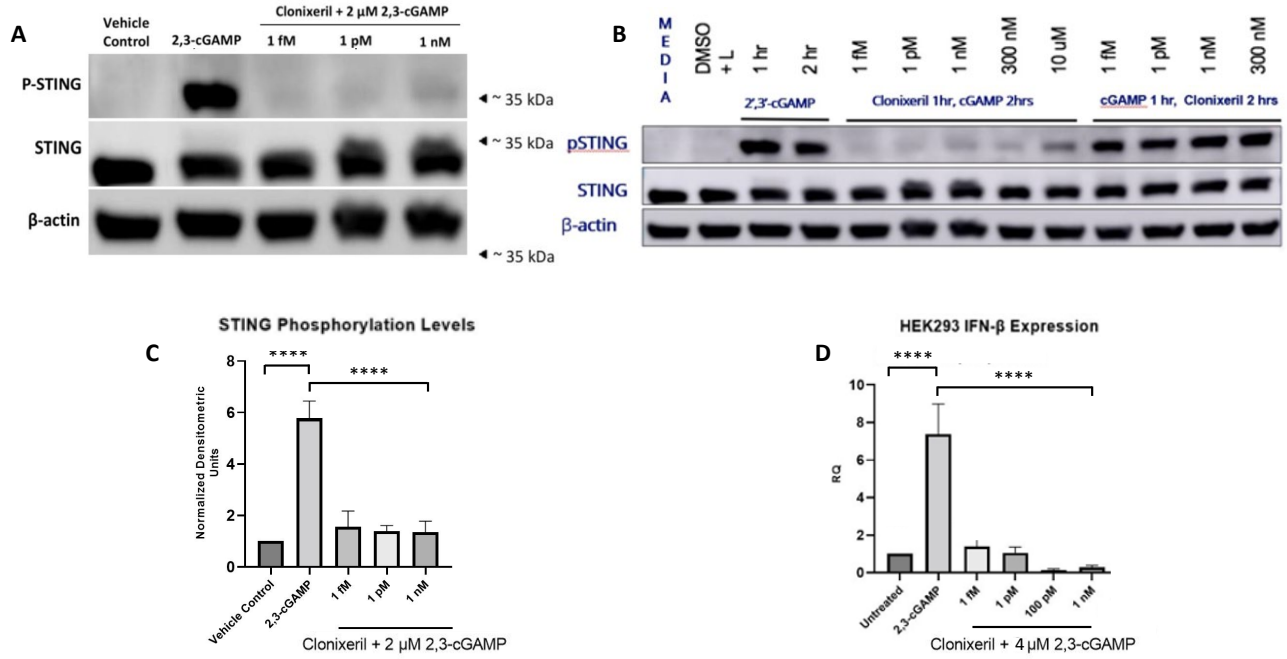

Figure 3. Effects of Clonixeril on STING phosphorylation and downstream IFN-β production. Western Blot analysis for STING and pSTING, qPCR of HEK293 treated with 2',3'-cGAMP and clonixeril, and clear native PAGE for STING. Data points were analyzed with a one-way ANOVA test using GraphPad Prism. (A) Western blot of HEK293 cells treated with various concentrations of clonixeril followed by treatment with 2 µM 2',3'-cGAMP; n=3**.** (B) Western blot of HEK293 cells treated with various concentrations of clonixeril followed by treatment with 2 µM 2',3'-cGAMP; n=3**.** (C) Quantitative analysis of Figure 3A. (D) qPCR data for IFNβ levels in HEK293 cells treated with various concentrations of clonixeril followed by treatment with 4 µM 2',3'-cGAMP; n=5.

Clonixeril Inhibits 2',3'-cGAMP-Dependent Production of IFN-β in HEK293 cells

Various genes comprise the IFN-1 family, including IFN-α, IFN-β, IFN-ω, -ε, and -κ.[31, 32] IRF3 activation leads to induction of a strong IFN-β response. Thus, we proceeded to evaluate whether CXL would affect IFN-β levels. HEK293 cells were treated with CXL (1 fM-1 nM) for 1 hour followed by 4 µM 2',3'-cGAMP for 3 hours. Cells treated with 4 µM 2',3'-cGAMP were used as a positive control. 4 µM 2',3'-cGAMP was an optimized dose based on a dose-response study for this experiment. IFN-β expression levels were measured using real-time qPCR. We observed a 7.4-fold induction of IFN-β production in the positive control group. All CXL treatment groups diminished 2',3'-cGAMP-induced expression of IFN-β by more than 50% including a concentration of 1 fM (**Figure 3D**).

Fluorescence Microscopy Experiments Suggest that CXL Affects hSTING Oligomerization

STING undergoes condensed *cis*-oligomerization as part of its signal transduction pathway and punctate structure formation of p-hSTING in the perinuclear region is indicative of hSTING oligomerization.[12] We had speculated that CXL might affect hSTING oligomerization. Hence, in a preliminary study we employed immunofluorescence to visualize how distribution of p-hSTING would be affected by treatment with CXL. HEK293 cells were treated with either 10 aM or 1 pM CXL for 1 hour followed by 2 μM 2',3'-cGAMP for 90 minutes. Cells treated with vehicle control for 1 hour and then 2 μM of 2',3'-cGAMP for 90 minutes were used as a positive control. At a 1 pM concentration of CXL, both p-hSTING and punctate structure formation were diminished. In addition, our results suggest that CXL treatment at a concentration of 10 aM may affect 2',3'-cGAMP induced p-hSTING puncta formation in the perinuclear region (**Figure S3**) but we cannot definitively claim that this is the case based upon these results. However, levels of hSTING phosphorylation were qualitatively unaffected by 10 aM CXL treatment.

In vitro Characterization of 2'3'-cGAMP's Effect on hSTING CTD Oligomerization Using Biophysical Methods

Dynamic Light Scattering (DLS) and Mass Photometry

Based upon our fluorescence microscopy studies **(Figure S3**), we hypothesized that CXL may affect hSTING oligomerization. DLS was used to determine how CXL affects our His-SUMO-TEV-hSTING CTD construct (subsequently referred to as SUMO-hSTING CTD). These STING oligomerization experiments were conducted under conditions in which 2',3'-cGAMP is present, as is the case for our competition experiments. The data presented in **Figure 4A** suggest that CXL alters the ability of SUMO-hSTING CTD to oligomerize in the presence of 2',3'-cGAMP. It is noteworthy that this effect is observed with concentrations of CXL as low as 100 aM. Interestingly, the interaction of CXL alone with SUMO-hSTING CTD causes a moderate amount of oligomerization within the same concentration range (**Figure 4B**). This observation demonstrates that CXL has a propensity to cause oligomerization on its own. Importantly, neither H-151, a known STING covalent antagonist that functions upstream of the CTD nor CXN showed reduction in 2',3'-cGAMP driven SUMO-hSTING

CTD oligomerization or an increase in SUMO-hSTING CTD oligomerization without 2',3'-cGAMP present (**Figure 4 A, B**). To support the premise that we were measuring STING CTD oligomers *via* DLS, we employed mass photometry, a different method for detection of protein oligomerization. Accordingly, SUMO-hSTING CTD alone and SUMO-hSTING CTD with 2',3'-cGAMP (at the same concentrations as used for our DLS experiments) showed results entirely consistent with our DLS studies.

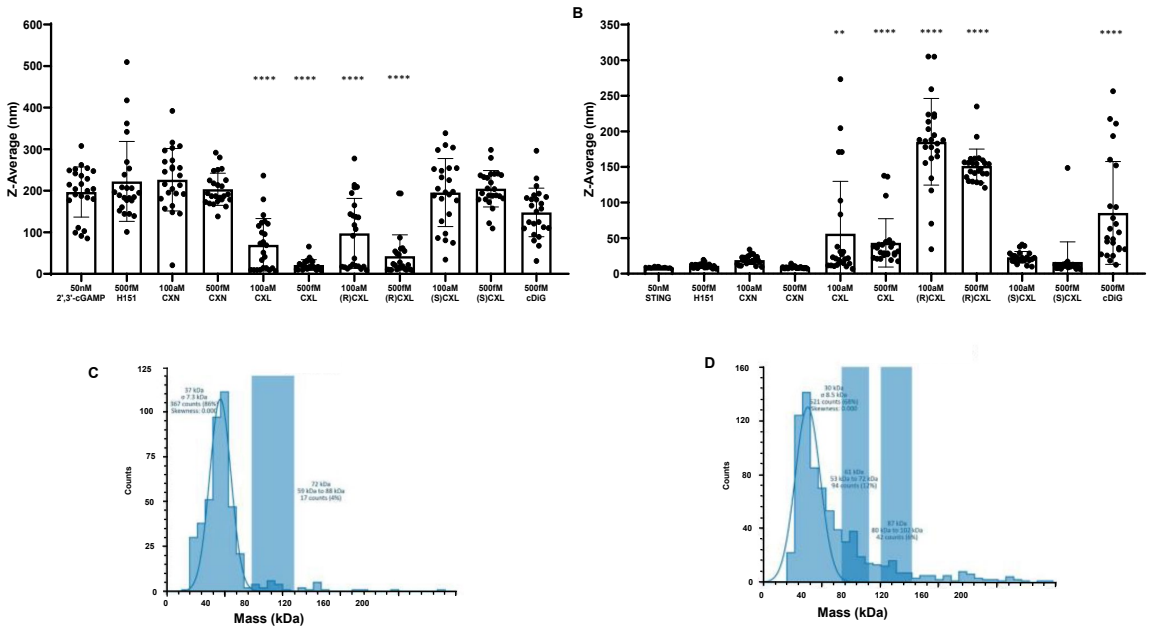

Figure 4. Dynamic light scattering and mass photometry measurements of STING oligomerization. (A) DLS was performed for 2 hours (n = 960 measurements) with 50 nM STING exposed to analytes. (B) Mass photometry of STING without 2',3'-cGAMP present. Blue blocks indicate size counts as a percentage to overall mass over selected mass ranges. (C) DLS was performed for 2 hours (n = 960 measurements) with 50 nM STING and 50 nM 2',3'-cGAMP exposed to analytes. (D) Mass photometry of STING exposed to 2',3'-cGAMP. **p-value <0.01; ****p-value <0.0001 via one way ANOVA test generated with GraphPad Prism.

Surface Plasmon Resonance (SPR)

To confirm whether CXL affected hSTING in the sub-femtomolar range, SPR studies were initiated to determine binding affinities of CXL and endogenous ligands relative to our His-hSTING CTD construct. We performed a control experiment by measuring 2',3'-cGAMP's binding affinity for hSTING CTD using an S-Series CMD5 chip. A K_D for 2',3'-cGAMP hSTING CTD was obtained (**Figure S4A, Table S1**) and determined to be 3.45 nM with a k_{on} of 1.54 x 10^6 +/- 3.1 x 10^4 (1/Ms) and a k_{off} of 5.93 x 10^{-3} +/- 6.6 x 10^{-5} (1/Ms), compared to the K_D of 3.79 nM reported via ITC.[7] The K_D of cyclic di-GMP (c-diGMP) was determined to be 4.78 +/- 1.65 μM (**Table S1**). These results are in agreement

with our molecular modeling prediction of 2.4 nM K_D for 2',3'-cGAMP and 6.4 μM K_D for c-diGMP (see Supporting Information, supplementary text and **Table S2**). We determined binding of CXL to hSTING CTD to be 430 ± 140 nM (**Table S1**, **Figure 5A**). We also examined CXN, which resulted in weaker affinity binding to hSTING CTD of approximately 637 nM (**Table S1; Figure 5B**). This result for CXL was puzzling given the obvious subnanomolar effect of CXL as shown in the *in cellulo* results. Thus, we attempted to obtain SPR data for the interaction between low concentrations of CXL (picomolar and below) and hSTING CTD bound to an SPR chip. Unfortunately, the RU differences were small compared to instrumental noise which accentuates the sensitivity limit of the SPR instrument.

Figure 5

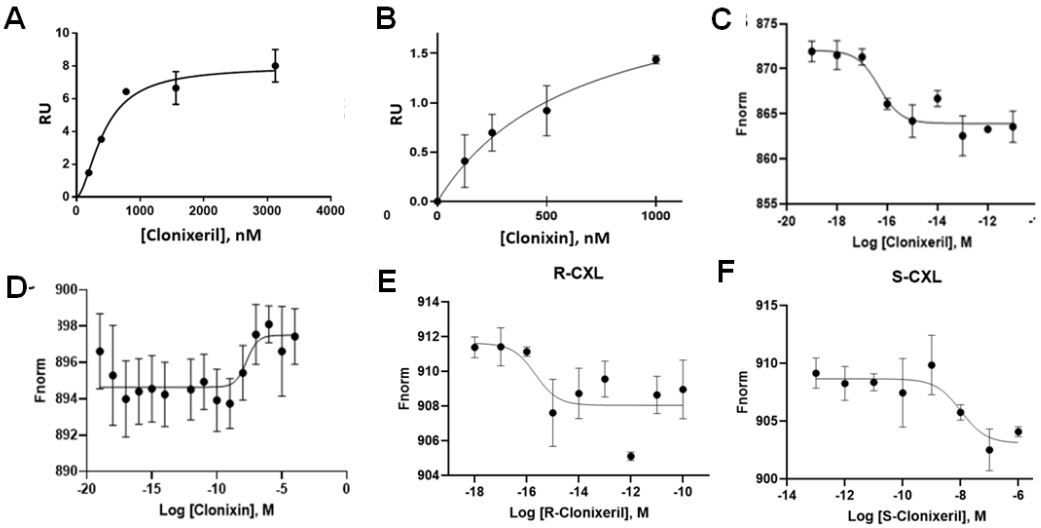

Figure 5. Surface Plasmon Resonance (SPR) and Microscale Thermophoresis (MST). (A) SPR analysis for clonixeril interaction from 187.5 nM to 6 μM without 2',3'-cGAMP present using STING CTD; (B) SPR analysis for clonixin interaction from 1 nM to 1 μM without 2',3'-cGAMP present using STING CTD; (C) MST analysis for clonixeril; titration shown is from 10 pM to 100 zM; N=3; p-value for shift <0.0061; (D) MST analysis for clonixin; titration shown is from to 100zM to 1 μM; N=3; p-value ns; (E) MST analysis for R-clonixeril; titration shown is from 1 aM to 100pM; N=3; (F) MST analysis for S-clonixeril; titration shown is from 100 fM to 1 μM; N=3.

Microscale Thermophoresis (MST) Studies

Next, we developed MST protocols that can reliably measure in the sub-femtomolar concentration range by leveraging the formation or disruption of presumed oligomer structures. Small molecule affinities at sub-picomolar concentrations are typically difficult to determine by MST due to the inability of the detector to measure differential movement of proteins when largely disproportionate ratios of protein to ligand are involved.[33] We developed a protocol that involves titrating hSTING CTD in the presence of 2',3'-cGAMP with a potential hSTING antagonist. We first performed a control experiment by titrating hSTING CTD with 2',3'-cGAMP. This experiment produced a K_d of 4.00 nM compared to

a reported K_d obtained by ITC of 3.79 nM.[7] We then titrated CXL into a STING/2',3'-cGAMP mixture, which presumably functions as a target for analyte interactions with oligomerized STING protein. This strategy provided the sensitivity needed to perform repeatable MST measurements with statistically significant thermal mobility. We determined that CXL possessed a sub-femtomolar EC_{50} (**Figure 5C**, EC_{50} <1fM). Generally, an IC_{50} correlates well with a K_D when a small molecule competes for binding with a natural substrate for a target protein.[34] We use EC_{50} here, though, because we contend that it is unlikely that simple binding is solely responsible for the activity we observe at very low concentrations (*vide infra*). Notably, CXN, the carboxylic acid precursor of CXL, gave an EC_{50} of approximately 500 nM (**Figure 5D**). This is consistent with the lower affinity interaction of CXN as measured by SPR (**Table S1, Figure 5B**). Based on our results with CXL and CXN, we synthesized a series of analogs in order to investigate structure activity relationships (SAR) of this chemotype (**Figure S5**). Through these experiments, we identified a closely related analog, mefenamic acid glycerol ester (**Figure 1A**), which surprisingly gave no indication of activity at any concentration below 1 μM, despite the fact that its chemical structure is nearly identical to CXL. This result emphasizes the fact that an SAR was established for CXL analogs in spite of the likelihood that we are not measuring a simple binding event at low concentrations.

Measurement of the interaction between CXL and hSTING CTD via Isothermal Calorimetry

In order to further explore the interaction between CXL and hSTING CTD, we employed Isothermal calorimetry (ITC) to measure the heat evolved accompanying CXL's effect on SUMO-hSTING^{WT} CTD. Given that we used a SUMO-hSTING CTD construct for these studies, we first attempted to reproduce the literature dissociation constant for the binding of c-diGMP to STING's CTD by ITC. In **Figure 6A**, we show the ITC data we obtained. Our ITC result for c-diGMP (K_d = 2.17 μM) is consistent with the value (3.70 μM) previously reported.[16] In **Figure 6B**, we show that the interaction of CXL with the hSTING CTD produces essentially the same amount of heat as c-diGMP at approximately the same final concentration, 400 μM (CXL) vs. 500 μM (c-diGMP). In **Figure 6B**, we also find that the binding isotherm is far from steady state or equilibrium, and thus we could not obtain reliable thermodynamic parameters. Nonetheless, a significant amount of heat was released in the process of CXL interacting with the hSTING CTD. On the other hand, we were most interested in ITC measurements taken at

femtomolar concentrations given the biophysical experiments and *in cellulo* studies already described. Initial experiments treating the hSTING CTD with femtomolar concentrations of CXL were unsuccessful, likely due to the insensitivity of the instrument. Thus, we resorted, as we had before in our MST studies, to competition experiments in which 2',3'-cGAMP was introduced into the reaction vessel along with the SUMO-hSTING CTD. In **Figure 6C** we show titration of 400 μM CXL into 40 μM SUMO-hSTING CTD in the presence of 20 μM 2',3'-cGAMP. This experiment produced similar amounts of heat as CXL alone (**Figure 6B**). A blank injection of aqueous DMSO to match the highest concentration of DMSO in CXL was titrated into 40 μM SUMO-hSTING CTD in the presence of 20 μM 2',3'-cGAMP (**Figure 6D)** to serve as a negative control, indicating that heat present in **Figure 6C** is the result of presence of CXL and not due to the DMSO or the interaction of DMSO with 2',3'-cGAMP. Comparable results to those depicted in **Figure 6D** were obtained when 2',3'-cGAMP was absent from the experiment (data not shown). In **Figure 6E**, 1.5 fM CXL was titrated into 40 μM SUMO-hSTING CTD in the presence of 20 μM 2',3'-cGAMP. This resulted in a significant evolution of heat in spite of the exceedingly low concentration of CXL.

Figure 6

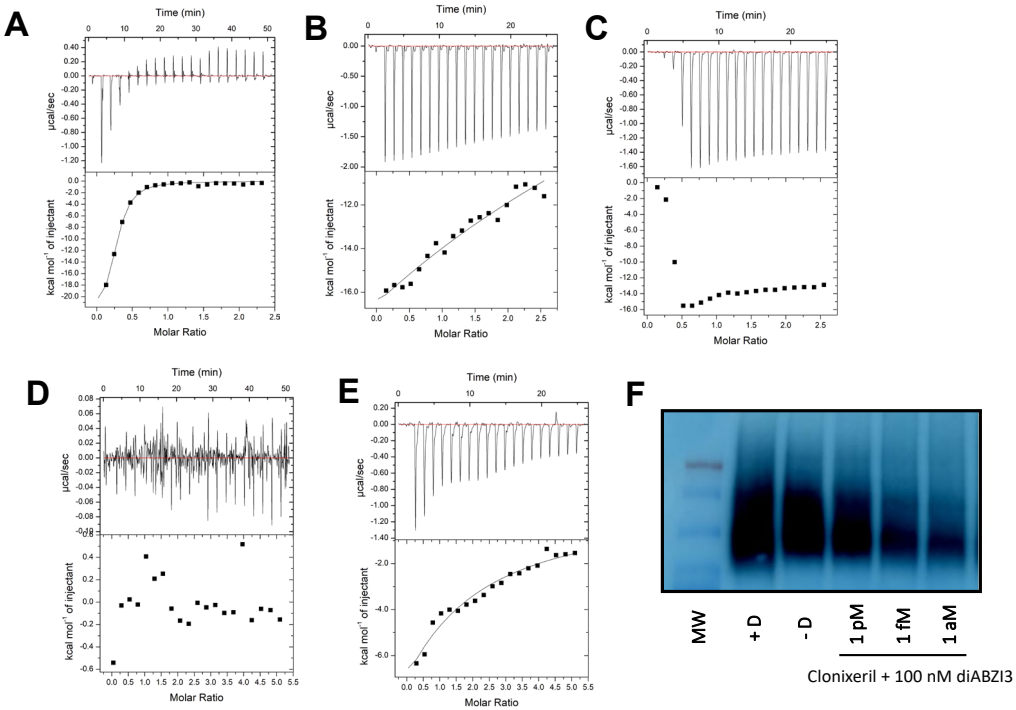

Figure 6. Isothermal Calorimetry of SUMO-hSTING^{WT} CTD and Clear Native PAGE; ITC analysis performed in HBS-P buffer. (A) Binding of 500 μM c-diGMP to 40 μM hSTING CTD. K_d = 2.17 μM; ΔH^o= -2.46*10^4 cal/mol; ΔS^o = -56.5 cal/mol/deg. (B) Binding of 400 μM clonixeril to 40 μM hSTING CTD. (C) Binding of 400 μM clonixeril to 40 μM hSTING CTD in the presence of 20 μM 2',3'-cGAMP. (D) Blank injection of DMSO into 40 μM hSTING CTD in the presence of 20 μM 2',3'-cGAMP. (E) Binding of 1.5 fM clonixeril to 40 μM hSTING CTD in the presence of 20 μM 2',3'-cGAMP. (F) Clear native PAGE of HEK293S cells treated with various concentrations of clonixeril followed by treatment with 100 nM diABZI3.

CXL inhibits hSTING oligomerization as demonstrated by Clear Native PAGE

To determine whether the results we observed in the DLS experiments could be recapitulated *in cellulo*, where full-length hSTING is present, we used HEK293T cells transfected with WT hSTING (referred to herein as HEK293S cells) to perform hSTING clear native PAGE experiments. Clear native PAGE is required because Coomassie Blue has been shown to disrupt STING oligomerization.[6] Thus, HEK293S cells were harvested following treatment with 100 nM diABZI3 for two hours, which was followed by a one hour treatment of varying concentrations of CXL. Our results demonstrate that CXL reduces hSTING oligomerization at concentrations down to attomolar levels with an inverse dose response (**Figure 6F)**. An inverse dose response is consistent with prior observations.

Clonixeril Enantiomers

It had not escaped our attention that the glycerol "tail" in the ester linkage of CXL, imparts chirality to CXL. Accordingly, we synthesized the two enantiomeric forms of CXL (**Supplementary Text**). Interestingly, in our MST assay, the R-enantiomer shows sub-femtomolar activity (**Figure 5E**), whereas the S-enantiomer seems to show an effect at higher concentrations (**Fig 5F**). We are currently investigating how the individual enantiomers behave *in cellulo.* In a preliminary study, the R-enantiomer, the S-enantiomer, and the racemic mixture were tested against HEK293S cells for which the hSTING pathway had been activated using diABZI3 and p-IRF3 was the measured end point by Westen blot (**Figure S7**). Interestingly, in this experiment, the R-enantiomer is agonistic at 100 fM, the S-enantiomer exhibits no effect at 100 fM, but it is the racemic mixture that exhibits potent antagonistic behavior at 100 fM. Interestingly, CXN appears to enhance the activity of diABZI3 (100 nM) at a concentration of 100 fM.

Discussion

We have demonstrated that CXL has unprecedented potency as a hSTING antagonist, while also exhibiting weak agonistic activity. In other words, it is a partial agonist. As it turns out, Ergun *et al.* have shown that unlike 2',3'-cGAMP, c-di-GMP activates the STING pathway by promoting protein

oligomerization without complete dimer angle closing.[35] They also demonstrated that, at sub-micromolar concentrations, c-di-GMP inhibits the action of 2',3'-cGAMP, with an approximate IC_{50} of 800 nM, meaning that c-di-GMP is also a partial agonist. Based on cooperativity observed for STING activation by c-di-GMP (Hill coefficient = 2.6), Ergun *et al.* proposed that c-di-GMP bound STING could oligomerize with apo-STING and this could result from the fact that they are conformationally similar (partially closed vs. open). In fact, as it turns out both conformations contain relatively closed dimer angles (*vide infra*). Ergun, *et al.* go on to propose that hetero-oligomerization increases the rigidity of the STING cyclic-dinucleotide binding site, which subsequently increases the affinity of STING for available c-di-GMP and gives rise to the observed cooperativity. Against that backdrop, we suggest that CXL, as a partial agonist, functions in a fashion similar to c-di-GMP but is a more potent antagonist by many orders of magnitude.

Recent cryo-EM studies reported by Liu, *et al.*, demonstrate that even full-length apo-STING itself is oligomerized (**Figure 1C**) to an extent and a manner that is very different from holo-STING (**Figure 1C**) and that full length apo-STING possess closed dimer angles relative to X-ray structures of apo-STING CTD.[16] Based upon the hetero-oligomerization described above involving the association of c-di-GMP bound STING with apo-STING, we speculate that CXL bound STING also interacts with apo-STING in its oligomerized state, and this serves to maintain autoinhibition. We suggest that this effect is non-stoichiometric, and only an exceedingly small number of CXL molecules are needed to stabilize the numerous oligomerized apo-STING molecules, and hence extremely low doses are needed to affect this type of antagonism. To further support this hypothesis, we have shown by DLS that CXL can prevent the hSTING CTD from forming high order oligomers *in vitro* upon simultaneous treatment with 2'3'-cGAMP, which is consistent with the model that CXL can prevent downstream oligomerization *in cellulo* caused by 2',3'-cGAMP. Finally, it is unlikely that CXL can reverse STING oligomerization downstream because this state is ultimately stabilized by disulfide crosslinking. This would explain why in our Western blot experiments involving p-hSTING formation using 2',3'-cGAMP as the activator (**Figure 3B**), CXL has no effect if HEK293 cells are treated with 2',3'-cGAMP prior to treatment with CXL. In that case, disulfide stabilized oligomers would not easily be disrupted. Finally, whereas we do not fully understand why

CXL seems to exhibit two distinct binding affinities, we suspect that CXL and c-di-GMP share a common mechanism by which this occurs. For reasons yet to be determined, at concentrations in the micromolar range they both behave as STING activators by presumably inducing productive oligomerization.

Given the extreme potency of CXL, as demonstrated by DLS, Mass Photometry, MST, and ITC techniques (all of which were applied to hSTING CTD; **Figures 4,5,6A-E**) and Clear Native PAGE, applied to full-length hSTING using HEK293S cell lysates (**Figure 6F**), it is unlikely that simple competitive binding of CXL to STING is sufficient to explain its extraordinary effects. It is noteworthy that our very first experiments using differential scanning fluorimetry resulted in a negative thermal shift. That fact suggests two things, (a) there is a protein ligand interaction taking place or there would be no thermal shift; (b) it is not a simple binding event, otherwise the shift would have been positive because the protein would have been stabilized against its thermal denaturation. Finally, it is very unlikely that all of our observations are the result of an artifact since if this was the case the artifact would have to be repeated across multiple types of *in vitro* and *in cellulo* experiments. To conclude, it is worth noting that our focus on the hSTING CTD for biophysical studies is substantiated by a study from Yin *et al.* illustrating the importance of the CTD in the hSTING oligomerization process initiated by c-diGMP.[36] We have, in fact, observed hSTING CTD oligomerization in the presence of c-diGMP using DLS. What is clear from our clear native PAGE experiments with HEK293S cells and DLS experiments using hSTING CTD is that CXL is affecting hSTING oligomerization, a necessary event for downstream signal transduction. This effect on oligomerization may be dependent on an initial binding event.

We find it intriguing that our ITC experiments have shown that when SUMO-hSTING CTD (pretreated with 2',3'-cGAMP) is exposed to CXL, a significant amount of heat is released even at a CXL concentration of 1.5 fM. This result demonstrates, at the very least, that a strong interaction has taken place between CXL and the hSTING CTD consistent with our MST observations. This experiment alone does not provide an indication of what that interaction is. That will hopefully be revealed by Cryo-EM studies. Nonetheless, it is astonishing that measurable heat is released at such a low analyte concentration. Moreover, it is unlikely that the heat release is due to a simple

binding event because we did not obtain an isotherm that is consistent with equilibrium binding thermodynamics. Again, it is tempting to speculate that CXL may engage STING in an initial simple binding event followed by a subsequent oligomerization or de-oligomerization event. In **Scheme 1** we provide a graphic representation of a possible mechanism that ties together all of the data and conjectures described above. **1. Observation**: When we treat HEK293 cells with 2',3'-cGAMP first, i.e., prior to treatment with CXL, little or no antagonism is observed. **Explanation:** This observation is consistent with the accepted mechanism for STING activation by 2',3'-cGAMP in which the disulfide bond formation in the oxidizing environment of the ER and Golgi causes the transduction to be irreversible (**Scheme 1A**). **2. Observation:** When we treat THP-1 cells with high concentrations of CXL alone, we observe agonism (**Figure 2A**). **Explanation:** CXL is a partial agonist like c-di-GMP, which causes partial closure of the STING dimer angles. We suggest that CXL, the glycerol ester of clonixin (CXN), may do the same at saturating concentrations (**Scheme 1B**). Moreover, we propose that the closely related compound, CXN (the carboxylic acid), only engages in the process shown in **Scheme 1B**. As previously stated, CXN appears to be weak agonist like CXL enhancing the activity of diABZI3 in our pIRF3 assay (**Figure S7**). Moreover, it only exhibits an inflection point by MST in the nanomolar range compared to CXL (**Figures 5C and D**) **3. Observation:** When we treat HEK293 and THP-1 cells with low concentrations of CXL prior to 2',3'-cGAMP we see potent antagonism. **Explanation:** Here we propose that CXL is binding to apo-STING, which is the autoinhibited state, but at low concentrations an unproductive oligomerization can occur when CXL occupied holo-STING oligomerizes with apo-STING non-stoichiometrically (**Scheme 1C**). This is a relatively stable inhibited state that cannot be reversed with 2',3'-cGAMP. It is likely that partially closed holo-STING stabilizes partially closed apo-STING and Ergun, *et al.* provide cryo-EM evidence for this hypothesis.[6, 35] **4. Why the inverse SAR?** Let's assume in **Scheme 1C**, which depicts the inhibited state, the concentration of CXL is 1 fM. The 2',3'-cGAMP signal is knocked down because 2',3'-cGAMP cannot disrupt the oligomers partially occupied by CXL. Note: in **Scheme 1C** the oligomers exhibit both *cis* and *trans* configurations with partial occupancy of CXL. Now let's assume that we have CXL at 1 pM concentration. Now the process shown in **Scheme 1B** begins to compete with the process depicted in **Scheme 1C**. 2',3'-cGAMP may also compete with the process shown in **Scheme 1B**, either way we would

observe reduced antagonism relative to CXL at 1 fM, which suggests an inverse dose response as seen in **Figures 2B, 2C**, **3B, 6F.** Notably, this paradoxical behavior has previously been observed for receptor-ligand interactions, but not for STING antagonists.[37]

Scheme 1

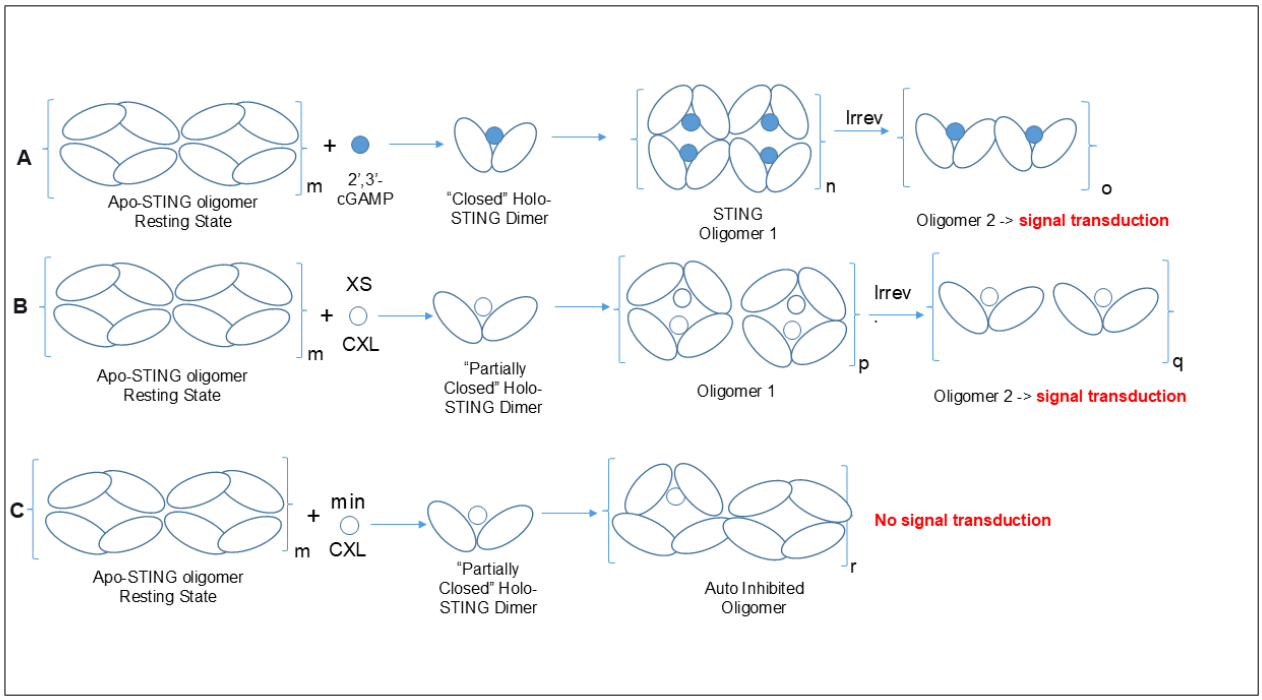

Scheme 1. Clonixeril (CXL); Excess (XS); min implies picomolar or lower concentrations. (A) The proposed mechanism for activation of STING by its endogenous ligand, 2',3'-cGAMP.[6] Note that a conformational change in the C-terminal tail (not shown) plays a role in exposing the protein oligomer surface upon binding of the ligand; not shown here for clarity. (B) Proposed mechanism for the agonist activity of CXL observed at micromolar concentrations.(C) Hypothetical mechanism for sub-picomolar antagonist activity of CXL.

We reiterate that we have observed the effects of CXL at below 1 fM. A simple calculation shows that at 1 fM, the number of molecules per THP-1 cell in our luciferase reporter assay is only approximately 3 molecules per cell. Whereas the number of STING molecules per cell is estimated to be between 300-1,000.[38] This ratio is perhaps a cause for concern but we cannot rule out that intercellular communication may be combined in some way with the extremely low concentration effects we observe in our biophysical studies. It is known that STING is degraded by cellular autophagy.[8] Might it be possible that autophagy induced intercellular communication stimulated by CXL is operative here?[39] The answer to this question will have to await further experimentation, which is currently underway in our laboratories.

Lastly, we note that CXL may be used as an oral drug in a clinical setting. We have shown that strikingly, it undergoes relatively slow hydrolysis at a pH of 1.0 (**Figure S4B**) and would be stable within the acidic environment in the human stomach. It has already been shown that oral administration of CXL in rats reduces inflammation. A dose of 30-300 mg/kg CXL in rats has anti-inflammatory effects without producing significant ulcerogenic effects.[40] We speculate that the findings we describe here could provide a novel breakthrough for the treatment of autoimmune diseases driven by modulation of STING activity. Should CXL itself not prove to be useful in a clinical setting, it could serve as a lead compound for further optimization. We have already synthesized over 40 CXL analogs that demonstrate an SAR by MST (**Figure S5**). They are currently being tested in our lab and the labs of our collaborators.

Conclusion

We have demonstrated that CXL is an extremely potent antagonist of the $hSTING^{WT}$ receptor and exhibits potencies not previously described for small molecule enzyme inhibitors or receptor antagonists, i.e., attomolar (10^{-18} M) levels. Two different hSTING activators (2',3'-cGAMP and diABZI3) have been employed to compete with CXL and similar results were obtained. Cell-based experiments were conducted in different laboratories in separate locations and by different personnel, and the results were the same.

In this manuscript, we propose a mechanism of action for CXL's modulatory effect on the STING pathway. We contend that the proposed mechanism is consistent with our data, where we have shown that CXL modulates STING oligomerization both *in vitro* and *in cellulo*. However, the precise mechanism at the atomistic level of detail for CXL's unprecedented potency as a STING antagonist will have to await Cryo-EM studies which are underway.

Experimental Section

Materials

THP1-Dual KI-hSTING-R232 cell lines were purchased from Invivogen (USA). HEK293 cells were purchased from American Type Culture Collection (ATCC). HEK293T cells were purchased from American Type Culture Collection (ATCC) and transfected with WT hSTING commercially available plasmid (pUNO1-; Invivogen); referred to as HEK293S cells. Roswell Park Memorial Institute (RPMI) 1640 media containing 25 mM 4-(2-hydroxyethyl)-1-piperazineethanesulfonic acid (HEPES) buffer, Dimethyl sulfoxide (DMSO), SyproOrange and 2 mM L-glutamine were purchased from Thermo Fisher Scientific (USA). Normocin™, Zeocin™, blasticidin penicillin-streptomycin antibiotics were purchased from Thermo Fisher Scientific (USA). Fetal bovine serum (FBS) was purchased from Gibco (USA). CXL was synthesized in house as described in the **Supplementary Text**. Mefenamic Acid Glycerol Ester was synthesized as described in the **Supplementary Text**. Ultrapure MilliQ water was given to us by the University of South Florida Geology Department (USA). QUANTI-Luc™ luminescence assay reagent, 6X-His tagged hSTING^{WT}, R232 variant, CTD protein was purchased from either Invivogen (USA) or Cayman Chemicals (USA). A Glowmax luminometer was obtained from Promega (USA). The Biacore T200 was obtained from GE Healthcare (USA). 2'3'-cGAMP were purchased from Cayman Chemicals (USA). For His-SUMO-TEV-hSTING CTD see Protein Production and Purification Methods.

Computational Methods

Protein Preparation for Computational Studies

Protein model systems of hSTING CTD variants are prepared using the Schrödinger, Inc. software suite. Protein structure coordinates were obtained from the Protein Data Bank (PDB). Models were generated from PDB entries: 4LOH (hSTING-CTD, H232 allele, 2'3'-cGAMP bound), 4LOI (hSTING-CTD, H232 allele, 2',2'-cGAMP bound), 4EMT (hSTING-CTD, WT allele, c-di-GMP bound), 4EMU (hSTING-CTD, WT allele, apo structure), 4KSY (hSTING-CTD, WT allele, 2'3'-cGAMP bound), and 4F5W (hSTING-CTD, HAQ allele, apo structure).

Molecular Dynamics for Virtual Screening

MD simulations were performed with the GPU accelerated Desmond MD program (available from Schrödinger, Inc.) on two Nvidia GeForce GTX 1080 Ti video cards. A cubic simulation box was created extending at least 10Å from the protein with imposed periodic boundary conditions using TIP3P waters [95] as solvent. The OPLS-3 all-atom force field was then applied to all atoms. Simulations were run at a temperature of 310 K and a constant pressure of 1 atm. All systems are energy minimized followed by multiple restrained minimizations to randomize systems before equilibration and final simulation. Production MD is performed on all systems for 250 ns. Final system equilibration is determined by the observation of asymptotic behavior of the potential energy, Root Mean Square Deviation (RMSD), and Radius of Gyration (Rg) profiles and visual inspection of trajectories guided by Root Mean Square Fluctuation (RMSF) profiles.

Computational Docking

After equilibrium is determined, a hierarchical average linkage clustering method based on RMSD was utilized to determine an average representative structure for the equilibrated hSTING systems. The representative structure is then used for consensus docking incorporating four complementary docking methods available in the Schrödinger, Inc. software suite: SP and XP rigid receptor docking, Induced Fit Docking, and Quantum Polarized Ligand Docking.

As a check for the placement of the GLIDE grids used in the docking studies and for further analysis of the binding cavity for the CDN binding site, Schrödinger's SiteMap program was employed. SiteMap searches the protein structure for likely binding sites and highlights regions within the binding site suitable for occupancy by hydrophobic groups, hydrogen-bond donors, acceptors, or metal-binding functionality of the ligand. All ligands were prepared using the program LigPrep and the OPLS-3 all-atom force field was applied to all ligand atoms.

Rigid Receptor Docking
Rigid docking simulations were performed by the docking program GLIDE (Schödinger, Inc.). GLIDE uses a GlideScore fitness function based on ChemScore for estimating binding affinity, but includes a steric-clash term, adds buried polar terms to penalize electrostatic mismatches, and modifies other secondary terms.

Cellular Assays

THP1 Luciferase Assays
STING THP1 Reporter Assay of IRF3 Promoter with Clonixeril as Agonist
QUANTI-Luc™luminesence Dual reporter THP1 cell assay was prepared according to the manufacturer's instructions (Invivogen, San Diego, CA, USA). A 10mM stock solution of CXL in 100% DMSO was diluted with ultrapure Milli Q water to make 3, 5, 10, 15, 20, 30, 40, 50μM samples. The vehicle control contained blank cell media treated with 0.1% DMSO. 20μL sample/well of CXL or dilute DMSO (vehicle control) was added to a white, 300μL, sterile 96 well plate. 180μL of reporter cells were then plated at 500,000 cells/mL and treated for 10h instead of the 18-24h incubation suggested by the manufacturer. These cells were resuspended in media with phenol red but without antibiotics, or phosphate-buffered saline (PBS), these two additives were found to cause statistically significant changes to results. All samples contained a final DMSO concentration of 0.1%. This concentration was found to be non-lethal to THP-1 cells in a cell viability assay. The expression of Lucia luciferase was quantified by measuring luminescence and evaluated in triplicate. Data are average luminescence changes shown as relative luminescence after subtraction of background luminescence of vehicle-treated cells. A Glowmax luminometer with an injector was used for measurement of luminescence in the luciferase assay. After the 10h incubation period, 20μL/well of cell culture supernatant was transferred to a fresh well plate. A single injector added 50 μL of detection reagent per well and immediately measured luminescence using a 4s incubation time integrated over 1 s.

STING THP1 Competition Assay of IRF3 Promoter with 2',3'-cGAMP as the Activator
The standard procedure from the vendor (Invivogen) for QUANTI-Luc™luminesence Dual reporter THP1 cell assay was modified for the competition of CXL with 2',3'-cGAMP. Thus, an 18-20 hr. incubation period, media with phenol red, cell density of five hundred thousand cells/mL, and 4μM 2',3'-cGAMP as the STING pathway activator were employed. A study was performed to determine that five hundred thousand cells/mL was the optimal cell density. An optimization study was performed to determine the maximum DMSO percentage so as to not impact the viability of the cells. The DMSO was kept at 0.1% or lower as this was the best concentration to keep the compound in solution and also not affect the viability of the cells. The two controls used in this experiment were media control, which was the standard media with no additives, and the vehicle control was the same percentage DMSO as in the experimental wells with media to establish a base line. 2',3'-cGAMP was tested at a variety of concentrations. The chosen concentration was 4μM. The cells were tested with lipofectamine and compared to wells prepared without lipofectamine. There was no significant difference between the two measurements, it was hypothesized that this is because THP-1 cell lines are known to be permeable to nucleotides like 2',3'-cGAMP. The optimal incubation time for the cells tested was from 1hr post the addition of 2',3'-cGAMP up to 24 hrs. post the addition of 2',3'-cGAMP. The optimal time for CXL occurred at 10 hrs. which included a 1 hr. pre-incubation time with the compound before the addition of 2',3'-cGAMP.

STING THP1 Inhibition Assay using diABZI3 as the Activator
The cells were grown in RPMI 1640, 2 mM L-glutamine, 25 mM HEPES, 10% heat-inactivated fetal bovine serum, 100 μg/mL Normocin, and Pen-Strep (100 U/mL−100 μg/ mL). For selection, the cells were passaged with and without addition of antibiotics (10 μg/mL of Blasticidin and 100 μg/mL of Zeocin) to the growth medium every other passage. Once the cells were confluent, they were pelleted and suspended in test medium containing: RPMI 1640, 2 mM L-glutamine, 25 mM HEPES, 10% heat-inactivated fetal bovine serum, and Pen-Strep (100 U/mL−100 μg/mL). The cells were counted in a cell counter to obtain a cell density of 1 × 106 cells/mL of test media. The cells were plated (25 μL) in

a 384-well Greiner plate (Cat. No. 781098). Compounds were generally dosed at final concentrations of 40, 20, 10, 5, 2.5, 1, 0.5, 0.25, 0.01, and 0.05 μM (1% DMSO final). After 1 h of incubation at 37 °C, 50 nM diABZI3. diABZI3 was added to all of the wells containing compounds and control wells. The negative control wells contained 1% DMSO. The cells were then incubated at 37°C for 24 h. QUANTI-Luc (Invivogen) reagent was then diluted in 30 mL of water, 75 μL was added to each well, and luminescence was read immediately (PerkinElmer Envision 2105). The data were normalized to the DMSO only controls (without diABZI3 or 2',3'-cGAMP), and percentage activation was calculated based on the diABZI3 or 2',3'-cGAMP only control. Compounds were dosed in triplicate.

HEK293 Assays

HEK293 pSTING Western Blot Analysis Using 2',3'-cGAMP

HEK293 cells were seeded at 700,000 cells per 60 mm plate confluency and treated 36 hours later. The samples were first treated with varying concentrations of CXL for 1 hour prior to 2 μM 2',3'-cGAMP (InvivoGen) for 1 hour and 30 minutes using Escort IV transfection reagent (Sigma Aldrich). 2 μM 2',3'-cGAMP was an optimized value based on a dose-response curve for this experiment. Vehicle control group was treated with Escort IV reagent and DMSO for 1 hour prior to 2 μM 2',3'-cGAMP (InvivoGen) for 1 hour and 30 minutes using Escort IV transfection reagent. DMSO concentration was kept constant across all treatment groups. Total cell lysates were collected and analyzed by Western blotting using antibodies against p-STING, STING, and β-actin. Experiments were repeated three times with comparable results. Data points were analyzed with a one-way ANOVA test using PRISM9 statistical analysis software (GraphPad). A level of $p < 0.05$ was considered statistically significant.

HEK293 Quantitative Real-Time (qPCR) for IFN-β

HEK293 cells were seeded at 700,000 cells per 60 mm plate confluency and treated 36 hours later. The samples were first transfected with varying concentrations of CXL for 1 hour prior to transfection with 4 μM 2',3'-cGAMP (Selleck Chem) for 3 hours using Escort IV transfection reagent (Sigma Aldrich). 4 μM 2',3'-cGAMP was an optimized value based on a dose-response curve for this experiment Total RNA was isolated using TRIzol (Invitrogen™) according to the manufacturer's instructions. iScript™ cDNA Synthesis Kit (Bio-Rad) was used to reverse-transcribe cDNA from 1 μg total RNA in accordance with manufacturer's protocol. SYBR Green real-time qPCR with IFN-β and GAPDH primers was performed for RQ using group treated with 2',3'-cGAMP alone as reference.

HEK293 Immunofluorescence

HEK293 cells were seeded into four-chambered slides (5,000 cells/well.) 36 hours later, sample 1 was first treated with vehicle control for 1 hour and then transfected with 2 μM 2',3'-cGAMP (InvivoGen) using Escort IV transfection reagent (Sigma Aldrich) for 1 hour and 30 minutes. Samples 2 and 3 were first transfected with 10 aM and 1 pM CXL, respectively, for 1 hour, followed by 2 μM 2',3'-cGAMP for 1 hour and 30 minutes. 2 μM 2',3'-cGAMP was an optimized value based on a dose-response curve for this experiment. DMSO concentration was kept constant across all treatment groups. Cells were fixed with 4% paraformaldehyde for 15 minutes and immuno-stained with p-STING antibody at 4°C overnight with light agitation. The slides were incubated with Alexa 594 rabbit secondary antibody for 1 hour at RT. Subsequently, the slides were stained with Phalloidin conjugated to FITC (488) for 30 minutes at RT, mounted with solution containing 4′,6'-diamidino-2-phenylindole (DAPI) and imaged on a Fluorescent Microscope.

His-SUMO-TEV-STING (SUMO-hSTING CTD) Protein Production and Purification

The gene encoding human STING (amino acid 155-343) was synthesized and subcloned into pET28a vector (Gift from Dr. Leemor Joshua-Tor of Cold Spring Harbor Laboratory, Huntington, NY) and expressed as N-terminal 6x His and SUMO duo tagged fusion protein in *E. coli* cell strain BL21(DE3). Cells were harvested 20 hours post induction by 0.5 mM IPTG and resuspended in lysis buffer containing 50 mM Tris, pH 7.5, 300 mM NaCl, 20 mM imidazole, 0.5 mM tris(2-carboxyethyl)phosphine (TCEP), 5% glycerol, 0.1% Triton X-100, 1 tablet of EDTA free protease inhibitor cocktail/50 mL lysis buffer. The supernatant of the cell lysate was applied to an XK 16 column (Cytiva) packed with Ni-NTA superflow resin (Qiagen), and the fusion protein was washed out by a liner gradient elution with a buffer composed of 50 mM Tris, pH 7.5, 300 mM NaCl, 500 mM imidazole, 0.5 mM TCEP, and 5% glycerol. The purified protein was analyzed by sodium dodecyl sulfate-

polyacrylamide gel electrophoresis (SDS-PAGE) (**Figure S8**), flash-frozen in liquid nitrogen, and stored at -80°C for further use.

Biophysical Assays

Dynamic Light Scattering

$hSTING^{WT}$ (His-tagged) protein or His-SumoTEV-hSTING protein was filtered using a 100 kDa centrifuge filter at 12,000 x g for 3 minutes and solubilized at 200nM in HBS-P (0.01M HEPES pH 7.4, 0.15 NaCl, 0.005% v/v surfactant P20). Concentration was reestablished via nanodrop using Ext. coefficient for His-SUMO-STING at 24870 M^{-1} cm^{-1}. Measurements were made using a Malvern Zetasizer Nano ZS set to 40 measurements at 1 s/measurement and 24 runs. Samples were created using 20 µL analyte with 10 µL protein and 10 µL 2',3'-cGAMP or buffer into a disposable low volume cuvette. The final concentration of all samples were 50 nM STING and 50 nM 2',3'-cGAMP with a titrated range of analyte.

Mass Photometry

Microscope coverslips were used in sample preparation for the mass photometry (Refeyn Two^{MP}) experiments, by washing three times with Milli-Q water followed by two isopropanol washes. The coverslip was then dried using an air can. Purified SUMO-hSTING CTD protein stock was diluted to 100 nM in a buffer containing 10 mM HEPES pH 7.4, 150 mM NaCl, 5% glycerol, and 0.5 mM TCEP. Twenty µL of each protein sample (100 nM) were incubated for 120 minutes with 1000 nM of either 2,3-cGAMP or Clonixeril or both. The control sample contained the hSTING CTD protein only. Two µl of each protein sample was added to the coverslip and loaded onto the instrument. A movie of 60 seconds was recorded. Data was analyzed using DiscoverMP software (Refeyn Two^{MP}).

Surface Plasmon Resonance (SPR)

SPR was employed for binding measurements using His-tagged $hSTING^{WT}$ CDN domain. A GE Healthcare Biacore T200 was equipped with a Ni-NTA chip. 16,951 RU of 6X-His tagged human STING was crosslinked via NHS chemistry following injections of 350 mM EDTA and 500 mM $NiSO_4$. STING natural substrates and the lead compound were titrated and flowed at 60 µL/min in 1X PBS for 60 sec association time followed by a 135 sec dissociation. The sensorgrams were analyzed using Biacore T200 Software 3.0 and steady state was measured at 4 sec before injection stop, exported into Graphpad, and fit versus concentration using a one site specific binding model to calculate the apparent equilibrium dissociation constant (K_D). Where appropriate, kinetics were measured using a 1:1 Langmuir binding model with R_{max} set to local to obtain the association rate (K_{on}), dissociation (K_{off})

Microscale Thermophoresis (MST)

STING R232 variant (human recombinant, wild-type) protein was solubilized at 200nM in HBS-P (0.01M HEPES pH 7.4, 0.15 NaCl, 0.005% v/v surfactant P20) along with 100 nM 2',3'-cGAMP. 100 nM of NTA-Atto 488 dye (blue; nitrilotriacetic acid complexed to Ni^{2+} - ion) is added and incubated for 1 hour at RT covered from light. The resulting mixture was centrifuged at 12,000 x RPM 10 minutes prior to use. A 1:10 series dilution from 200mM to 200zM was created using HBS-P with 1% DMSO. The dyed STING/2',3'-cGAMP mixture was added to each sample in a 1:1 ratio, resulting in a static 100 nM STING, 50 nM 2',3'-cGAMP, and a concentration range from 100 mM to 100 zM. Samples were incubated for 15 minutes prior to loading into Monolith NT.115 capillaries and run on NanoTemper Pico instrument. The samples were run again at 30- and 45-minutes. Detection of the protein was performed using the blue detection channel with excitation power set to 100% and MST set to high allowing 3 s prior to MST on to check for initial fluorescence differences, 35 s for thermophoresis, and 3 s for regeneration after MST off. Analysis was performed using M.O. Affinity Analysis Software with difference between initial fluorescence measured in the first 5 s as compared with thermophoresis at 30 s at 16 different analyte concentrations ranging from 100 mM to 100 zM and exported into Graphpad Prism v.8 using a Log inhibitor versus response for parameter fit. MST Confidence Intervals
for clonixeril. From Top 871.7 to Bottom 864.0; logIC50 -16.28; Hillslope -1.669; Span 7.723; Degrees of Freedom 5; R squared 0.9033; Sum of Squares 11.55; Sy.x 1.520.

Isothermal Titration Calorimetry (ITC)
Sumo-tagged recombinantly purified STING was used on a MicroCal PEAQ-ITC and analysis was performed using (Tim). Briefly, STING from -80 aliquots was spun down at 10,000 RPM for 5 minutes and loaded using a Hamilton syringe. Samples contained either 40 μM STING or 40 μM STING and 20 μM 23cGAMP. HBS-P buffer was utilized in 5% DMSO.

MicroCal ITC200 instrument (Malvern Pananalytical) was used to assess STING and CXL interactions. Both recombinantly purified STING domain (residues 155-343) containing a SUMO tag and CXL were buffer-exchanged and made in the same buffer composition, respectively, to avoid buffer mismatch. The same buffer cocktail was used in all ITC experiments, containing 25 mM HEPES, pH 7.4, 150 mM NaCl, 5% glycerol, 0.5 mM TCEP, and 5% DMSO. STING protein from -80°C aliquots was spun down at 12,000 RPM for 5-10 minutes before each run to remove any aggregates, diluted into the ITC buffer above (either as 40 μM STING alone or as 40 μM STING plus 20 μM 2,3-cGAMP), and loaded into the cell. CXL at various concentrations for different experiments was loaded into the syringe (Hamilton). For the control and reference, ITC buffer devoid of CXL was used. ITC experiments were conducted at 25 °C using an initial 0.4 μL injection and 19 subsequent injections of 2 μL each at 150 second intervals. Heat of dilution (differential power) of the 19 injections resulted from the binding event was fitted into the nonlinear least squares equation incorporated in the MicroCal ITC200 analysis software. The Kd and other thermodynamic parameters were derived from curve fitting using the MicroCal software.

Clear Native PAGE
Invitrogen™ NativePAGE™ Sample Prep Kit **Catalog number:** BN2008, Invitrogen™ NativePAGE™ Running Buffer Kit **Catalog number:** BN2007 and Invitrogen™ NativePAGE™ 4 to 16%, Bis-Tris, 1.0 mm, Mini Protein Gels, 10 wells, (Cat. # BN1002BOX). Cells were harvested and CXL was added at varying concentrations for 1 hour and followed by 2 hours of diABZI3 at 100 nM. To the mammalian cells harvested in 1 mL cell culture, add 0.2 mL lysis buffer containing 10 mM HEPES, pH 7.5,150 mM NaCl, 5% glycerol, protease inhibitor cocktail, and 0.025% digitonin. Cells were lysed by sonicating for two rounds of 15 seconds each while cooling the sample on ice. Centrifuge the lysate at 20,000 × g for 10 minutes at 4°C. Aliquot the supernatant into microcentrifuge tubes. To prepare the sample for loading a total volume of 20 μL NativePAGE™ including Sample Buffer (4X) 5 μLSTING supernatant, 14.5 μL and Ponceau S-dye: 0.5 μL. 1X NativePAGE™ Anode Buffer: Add 30 mL of 20X NativePAGE™ Running Buffer to 570 mL of deionized water. 1X NativePAGE™ Light Blue Cathode Buffer: Add 10 mL 20X NativePAGE™ Running Buffer and 1 mL 20X NativePAGE™ Cathode Additive to 189 mL deionized water. The gel was run at 150 V constant for 110 minutes. Gel was developed using A western blot using a PVDF transfer membrane was performed by the eBlot L1 Protein Transfer System.

Data and Material Availability

All data to understand and assess the conclusions of this research are available in the main manuscript or within the Supporting Information. Analog compounds pertaining to CXL are under patent consideration and therefore are not available for transfer. The synthetic scheme used for CXL is included in the Supporting Information.

Supporting Information

The Supporting Information is available free of charge at xxx.

Supplemental Text along with supplemental figures and tables referenced in the main manuscript or in the Supplemental Text are provided.

Author Information

Corresponding Author

Wayne C. Guida - *Department of Chemistry, University of South Florida, Tampa, Florida, 33620, United States; https://orcid.org/0000-0003-3353-4853; email wguida@usf.edu*

Authors

Robert Sparks - *Department of Chemistry, University of South Florida, Tampa, Florida, 33620, United States; Current address: Division of Gastroenterology, Department of Medicine; University of Massachusetts Chan Medical School, Worcester, Massachusetts, 01655, United States.*

William Lawless - *Department of Chemistry; University of South Florida, Tampa, Florida, 33620, United States; Current address: Department of Molecular Medicine, Morsani College of Medicine; University of South Florida, Tampa, Florida, 33620, United States.*

Anna Kharitonova - *Department of Chemistry; University of South Florida, Tampa, Florida, 33620, United States.*

Rainer Metcalf - *Department of Chemistry; University of South Florida, Tampa, Florida, 33620, United States. Current Address: Asha Therapeutics, LLC; USF Connect, Research & Innovation, Tampa, Florida, 33612, United States.*

Jamie Nunziata - *Department of Chemistry; University of South Florida, Tampa, Florida, 33620, United States.*

Grace A. Binder - *Department of Chemistry; University of South Florida, Tampa, Florida, 33620, United States.*

Sauradip Chaudhuri - *Biochemistry and Molecular Biotechnology Department; University of Massachusetts Chan Medical School, Worcester, Massachusetts, 01655, United States.*

Christine S.R. Gambino - *Department of Chemistry; University of South Florida, Tampa, Florida, 33620, United States.*

Michelle Wilde - *Department of Chemistry; University of South Florida, Tampa, Florida, 33620, United States.*

Linette S. Harding - *Department of Chemistry; University of South Florida, Tampa, Florida, 33620, United States.*

Jaret J. Crews - *Department of Chemistry; University of South Florida, Tampa, Florida, 33620, United States.*

Mansi Gopu - *Department of Chemistry; University of South Florida, Tampa, Florida, 33620, United States.*

Emilia Dalamangas - *Department of Chemistry; University of South Florida, Tampa, Florida, 33620, United States.*

Sarah Lawless - *Department of Molecular Medicine, Morsani College of Medicine; University of South Florida, Tampa, Florida, 33620, United States.*

Mark Eschenfelder - *Department of Chemistry; University of South Florida, Tampa, Florida, 33620, United States.*

Robert M. Green - *Biochemistry and Molecular Biotechnology Department; University of Massachusetts Chan Medical School, Worcester, Massachusetts, 01655, United States.*

Elizabeth X. Nompleggi - *Division of Gastroenterology, Department of Medicine; University of Massachusetts Chan Medical School, Worcester, Massachusetts, 01655, United States.*

Timothy Tran - *H. Lee Moffitt Cancer Center, Research Institute at the University of South Florida; Tampa, Florida, 33612, United States.*

Kathy Yang - *H. Lee Moffitt Cancer Center, Research Institute at the University of South Florida; Tampa, Florida, 33612, United States.*

Donna V. Trask - *Department of Chemistry; University of South Florida, Tampa, Florida, 33620, United States.*

Paul R. Thompson - *Biochemistry and Molecular Biotechnology Department; University of Massachusetts Chan Medical School, Worcester, Massachusetts, 01655, United States.*

Rekha Patel - *Research Service; James A. Haley Veterans Hospital, Tampa, Florida, 33612, United States.*

Niketa A. Patel - *Research Service; James A. Haley Veterans Hospital, Tampa, Florida, 33612, United States.*

Wesley H. Brooks - *Department of Chemistry; University of South Florida, Tampa, Florida, 33620, United States.*

W. Guy Bradley - Tampa Bay Research Institute, St. Petersburg, Florida, 33716, United States.

Mildred E. Acevedo-Duncan - *Department of Chemistry; University of South Florida, Tampa, Florida, 33620, United States.*

Alan C. Mullen - *Division of Gastroenterology, Department of Medicine; University of Massachusetts Chan Medical School, Worcester, Massachusetts, 01655, United States.*

James W. Leahy - *Department of Chemistry; University of South Florida, Tampa, Florida, 33620, United States.*

Kenyon G. Daniel - *Department of Chemistry; University of South Florida, Tampa, Florida, 33620, United States.*

Author Contributions:

Conceptualization: RPS, RM, PRT, ACM, JWL, KGD, WCG

Methodology: AK, WL, RM, RPS, MEAD, CSRG, NAP, JN, TT, RP, JWL, KY, WCB, KGD, WCG

Investigation: AK, WL, RM, RPS, MEAD, GAB, JJC, SC, RMG, ED, EXN, RMG, CSRG, MG, MW, ED, LSH, JN, TT, DVT, RP, SL, ME.

Visualization: AK, WL, RM, RPS, GAB, CSRG, LSH, JJC, TT, KY, KGD, WCG

Funding acquisition: WHB, KGD, JWL, WCG

Project administration: WHB, JWL, KGD, WCG

Supervision: PRT, ACM, JWL, KGD, WCG

Writing – original draft: AK, WL, RM, RPS, GAB, KGD, WCG

Writing – review & editing: AK, WL, RPS, ACM, JWL, KGD, WCG

Acknowledgements: We thank University of South Florida Chemical Purification, Analysis, and Screening Core and H. Lee Moffitt Cancer Center and Research Institute Chemical Biology Core. We thank Dr. P.K. Burnette, Scientific Director, Precision Medicine Oncology, AbbVie, Chicago, Dr. Peter T. Meinke, Sanders Director, Tri-Institutional Therapeutics Discovery Institute, NYC, and Mr. Sam Shrivastava, IBIS Therapeutics, LLC, for many helpful discussions about this work. We thank Dr. Leemor Joshua-Tor of Cold Spring Harbor Laboratory, Huntington, NY, for the generous gift of STING CTD plasmids. We thank Dr. Thomas Tuschl and Dr. Lodoe Lama of Rockefeller University, NYC for sharing their RNAseq data with us**.** Also, we thank Lennard Barasa for his inspiring conversations at UMass Chan Medical School.

Funding: This work was supported in part by The National Institutes of Health, National Institute for Allergy and Infectious Disease, R21AI149450. “Development of antagonists targeting STING in systemic lupus erythematosus,” 01/2020 – 12/31/2021 and in part by IBIS Therapeutic LLC. We thank both of them for their generous support.

Competing interests: Drs. Wesley H. Brooks, Kenyon G. Daniel, and Wayne C. Guida all have a financial interest in IBIS Therapeutics, LLC. Dr. Rainer Metcalf is a consultant for IBIS Therapeutics, LLC.

Patent WO2021042024A1, STING modulators, compositions, and methods of use. 2020.
Wayne C. Guida, Kenyon G. Daniel, Wesley H. Brooks, Linette Harding, Rainer Metcalf, Sam G. Shrivastava, James Leahy, and Robert P. Sparks.

:

References and Notes:

(1) Ablasser, A.; Chen, Z. J. cGAS in action: Expanding roles in immunity and inflammation. *Science* **2019**, *363* (6431), eaat8657. DOI: doi:10.1126/science.aat8657.
(2) Sun, L.; Wu, J.; Du, F.; Chen, X.; Chen, Z. J. Cyclic GMP-AMP Synthase Is a Cytosolic DNA Sensor That Activates the Type I Interferon Pathway. *Science* **2013**, *339* (6121), 786-791. DOI: doi:10.1126/science.1232458.
(3) Kuchta, K.; Knizewski, L.; Wyrwicz, L. S.; Rychlewski, L.; Ginalski, K. Comprehensive classification of nucleotidyltransferase fold proteins: identification of novel families and their representatives in human. *Nucleic Acids Research* **2009**, *37* (22), 7701-7714. DOI: 10.1093/nar/gkp854 (acccessed 6/30/2022).
(4) Gao, D.; Li, T.; Li, X.-D.; Chen, X.; Li, Q.-Z.; Wight-Carter, M.; Chen, Z. J. Activation of cyclic GMP-AMP synthase by self-DNA causes autoimmune diseases. *Proceedings of the National Academy of Sciences* **2015**, *112* (42), E5699-E5705. DOI: doi:10.1073/pnas.1516465112.
(5) Shang, G.; Zhang, C.; Chen, Z. J.; Bai, X.-c.; Zhang, X. Cryo-EM structures of STING reveal its mechanism of activation by cyclic GMP–AMP. *Nature* **2019**, *567* (7748), 389-393. DOI: 10.1038/s41586-019-0998-5.
(6) Liu, S.; Yang, B.; Hou, Y.; Cui, K.; Yang, X.; Li, X.; Chen, L.; Liu, S.; Zhang, Z.; Jia, Y.; et al. The mechanism of STING autoinhibition and activation. *Molecular Cell* **2023**, *83* (9), 1502-1518.e1510. DOI: https://doi.org/10.1016/j.molcel.2023.03.029.
(7) Zhang, X.; Shi, H.; Wu, J.; Zhang, X.; Sun, L.; Chen, C.; Chen, Zhijian J. Cyclic GMP-AMP Containing Mixed Phosphodiester Linkages Is An Endogenous High-Affinity Ligand for STING. *Molecular Cell* **2013**, *51* (2), 226-235. DOI: 10.1016/j.molcel.2013.05.022 (acccessed 2022/06/30).
(8) Zhang, K.; Wang, S.; Gou, H.; Zhang, J.; Li, C. Crosstalk Between Autophagy and the cGAS–STING Signaling Pathway in Type I Interferon Production. *Frontiers in Cell and Developmental Biology* **2021**, *9*, Mini Review. DOI: 10.3389/fcell.2021.748485.
(9) Zhang, R.; Kang, R.; Tang, D. The STING1 network regulates autophagy and cell death. *Signal Transduct Target Ther* **2021**, *6* (1), 208. DOI: 10.1038/s41392-021-00613-4 From NLM.
(10) Srikanth, S.; Woo, J. S.; Wu, B.; El-Sherbiny, Y. M.; Leung, J.; Chupradit, K.; Rice, L.; Seo, G. J.; Calmettes, G.; Ramakrishna, C.; et al. The Ca2+ sensor STIM1 regulates the type I interferon response by retaining the signaling adaptor STING at the endoplasmic reticulum. *Nature Immunology* **2019**, *20* (2), 152-162. DOI: 10.1038/s41590-018-0287-8.
(11) Ishikawa, H.; Barber, G. N. STING is an endoplasmic reticulum adaptor that facilitates innate immune signalling. *Nature* **2008**, *455* (7213), 674-678. DOI: 10.1038/nature07317.
(12) Zhang, C.; Shang, G.; Gui, X.; Zhang, X.; Bai, X.-c.; Chen, Z. J. Structural basis of STING binding with and phosphorylation by TBK1. *Nature* **2019**, *567* (7748), 394-398. DOI: 10.1038/s41586-019-1000-2.
(13) Zhao, B.; Du, F.; Xu, P.; Shu, C.; Sankaran, B.; Bell, S. L.; Liu, M.; Lei, Y.; Gao, X.; Fu, X.; et al. A conserved PLPLRT/SD motif of STING mediates the recruitment and activation of TBK1. *Nature* **2019**, *569* (7758), 718-722. DOI: 10.1038/s41586-019-1228-x.
(14) Zhao, B.; Shu, C.; Gao, X.; Sankaran, B.; Du, F.; Shelton, C. L.; Herr, A. B.; Ji, J.-Y.; Li, P. Structural basis for concerted recruitment and activation of IRF-3 by innate immune adaptor proteins. *Proceedings of the National Academy of Sciences* **2016**, *113* (24), E3403-E3412. DOI: doi:10.1073/pnas.1603269113.
(15) Liu, S.; Cai, X.; Wu, J.; Cong, Q.; Chen, X.; Li, T.; Du, F.; Ren, J.; Wu, Y.-T.; Grishin, N. V.; et al. Phosphorylation of innate immune adaptor proteins MAVS, STING, and TRIF induces IRF3 activation. *Science* **2015**, *347* (6227), aaa2630. DOI: doi:10.1126/science.aaa2630.
(16) Shang, G.; Zhu, D.; Li, N.; Zhang, J.; Zhu, C.; Lu, D.; Liu, C.; Yu, Q.; Zhao, Y.; Xu, S.; et al. Crystal structures of STING protein reveal basis for recognition of cyclic di-GMP. *Nature Structural & Molecular Biology* **2012**, *19* (7), 725-727. DOI: 10.1038/nsmb.2332.

(17) Shi, H.; Wu, J.; Chen, Z.; Chen, C. Molecular basis for the specific recognition of the metazoan cyclic GMP-AMP by the innate immune adaptor protein STING. *Proceedings of the National Academy of Sciences of the United States of America* **2015**, *112*. DOI: 10.1073/pnas.1507317112.
(18) Hopfner, K.-P.; Hornung, V. Molecular mechanisms and cellular functions of cGAS-STING signalling. *Nature Reviews Molecular Cell Biology* **2020**, *21*, 501+, Report. (acccessed 2022/8/4/). From Gale Gale OneFile: Health and Medicine.
(19) Dobbs, N.; Burnaevskiy, N.; Chen, D.; Gonugunta, V. K.; Alto, N. M.; Yan, N. STING Activation by Translocation from the ER Is Associated with Infection and Autoinflammatory Disease. *Cell Host Microbe* **2015**, *18* (2), 157-168. DOI: 10.1016/j.chom.2015.07.001 From NLM.
(20) Kemmoku, H.; Takahashi, K.; Mukai, K.; Mori, T.; Hirosawa, K. M.; Kiku, F.; Uchida, Y.; Kuchitsu, Y.; Nishioka, Y.; Sawa, M.; et al. Single-molecule localization microscopy reveals STING clustering at the trans-Golgi network through palmitoylation-dependent accumulation of cholesterol. *Nat Commun* **2024**, *15* (1), 220. DOI: 10.1038/s41467-023-44317-5 From NLM.
(21) Domizio, J. D.; Gulen, M. F.; Saidoune, F.; Thacker, V. V.; Yatim, A.; Sharma, K.; Nass, T.; Guenova, E.; Schaller, M.; Conrad, C.; et al. The cGAS–STING pathway drives type I IFN immunopathology in COVID-19. *Nature* **2022**, *603* (7899), 145-151. DOI: 10.1038/s41586-022-04421-w.
(22) Scozzi, D.; Cano, M.; Ma, L.; Zhou, D.; Zhu, J. H.; O'Halloran, J. A.; Goss, C.; Rauseo, A. M.; Liu, Z.; Sahu, S. K.; et al. Circulating mitochondrial DNA is an early indicator of severe illness and mortality from COVID-19. *JCI Insight* **2021**, *6* (4). DOI: 10.1172/jci.insight.143299 From NLM.
(23) Humphries, F.; Shmuel-Galia, L.; Jiang, Z.; Wilson, R.; Landis, P.; Ng, S. L.; Parsi, K. M.; Maehr, R.; Cruz, J.; Morales-Ramos, A.; et al. A diamidobenzimidazole STING agonist protects against SARS-CoV-2 infection. *Sci Immunol* **2021**, *6* (59). DOI: 10.1126/sciimmunol.abi9002 From NLM.
(24) Decout, A.; Katz, J. D.; Venkatraman, S.; Ablasser, A. The cGAS–STING pathway as a therapeutic target in inflammatory diseases. *Nature Reviews Immunology* **2021**, *21* (9), 548-569. DOI: 10.1038/s41577-021-00524-z.
(25) Li, Q.; Tian, S.; Liang, J.; Fan, J.; Lai, J.; Chen, Q. Therapeutic Development by Targeting the cGAS-STING Pathway in Autoimmune Disease and Cancer. *Frontiers in Pharmacology* **2021**, *12*, Review. DOI: 10.3389/fphar.2021.779425.
(26) Meng, X. Y.; Zhang, H. X.; Mezei, M.; Cui, M. Molecular docking: a powerful approach for structure-based drug discovery. *Curr Comput Aided Drug Des* **2011**, *7* (2), 146-157. DOI: 10.2174/157340911795677602 From NLM.
(27) Koes, D. R.; Camacho, C. J. Pharmer: efficient and exact pharmacophore search. *J Chem Inf Model* **2011**, *51* (6), 1307-1314. DOI: 10.1021/ci200097m From NLM.
(28) Irwin, J. J.; Shoichet, B. K. ZINC - A free database of commercially available compounds for virtual screening. *Journal of Chemical Information and Modeling* **2005**, *45* (1), 177-182. DOI: 10.1021/ci049714+.
(29) Humphries, F.; Shmuel-Galia, L.; Jiang, Z.; Zhou, J. Y.; Barasa, L.; Mondal, S.; Wilson, R.; Sultana, N.; Shaffer, S. A.; Ng, S. L.; et al. Targeting STING oligomerization with small-molecule inhibitors. *Proc Natl Acad Sci U S A* **2023**, *120* (33), e2305420120. DOI: 10.1073/pnas.2305420120 From NLM.
(30) Li, L.; Yin, Q.; Kuss, P.; Maliga, Z.; Millán, J. L.; Wu, H.; Mitchison, T. J. Hydrolysis of 2'3'-cGAMP by ENPP1 and design of nonhydrolyzable analogs. *Nat Chem Biol* **2014**, *10* (12), 1043-1048. DOI: 10.1038/nchembio.1661 From NLM.
(31) Taniguchi, T.; Mantei, N.; Schwarzstein, M.; Nagata, S.; Muramatsu, M.; Weissmann, C. Human leukocyte and fibroblast interferons are structurally related. *Nature* **1980**, *285* (5766), 547-549. DOI: 10.1038/285547a0.
(32) Pestka, S.; Krause, C. D.; Walter, M. R. Interferons, interferon-like cytokines, and their receptors. *Immunological Reviews* **2004**, *202* (1), 8-32. DOI: https://doi.org/10.1111/j.0105-2896.2004.00204.x.

(33) NanoTemper. *User Manual Monolith NT.115*. 2023. https://www.isbg.fr/IMG/pdf/manual_nt115_new.pdf (accessed 2023 September 7).
(34) Munson, P. J.; Rodbard, D. An exact correction to the "Cheng-Prusoff" correction. *J Recept Res* **1988**, *8* (1-4), 533-546. DOI: 10.3109/10799898809049010 From NLM.
(35) Ergun, S. L.; Fernandez, D.; Weiss, T. M.; Li, L. STING Polymer Structure Reveals Mechanisms for Activation, Hyperactivation, and Inhibition. *Cell* **2019**, *178* (2), 290-301.e210. DOI: 10.1016/j.cell.2019.05.036 (acccessed 2024/09/23).
(36) Yin, Q.; Tian, Y.; Kabaleeswaran, V.; Jiang, X.; Tu, D.; Eck, Michael J.; Chen, Zhijian J.; Wu, H. Cyclic di-GMP Sensing via the Innate Immune Signaling Protein STING. *Molecular Cell* **2012**, *46* (6), 735-745. DOI: 10.1016/j.molcel.2012.05.029 (acccessed 2022/06/30).
(37) Ritter, J.; Flower, R. J.; Henderson, G.; Loke, Y. K.; MacEwan, D. J.; Rang, H. P. *Rang and Dale's Pharmacology*; Elsevier, 2024.
(38) Tuschel, T., Lama, L. RNASeq data from THP-1 cells provided by Dr. Thomas Tuschl and Dr. Lodoe Lama, Rockefeller University.
(39) Piletic, K.; Alsaleh, G.; Simon, A. K. Autophagy orchestrates the crosstalk between cells and organs. *EMBO Rep* **2023**, *24* (9), e57289. DOI: 10.15252/embr.202357289 From NLM.
(40) Sherlock, M. H. Glyceryl, 2-(x,y,z-SUBSTITUTED ANILINO NICOTINATES, U.S. Patent No. 3,478,040. 1967.

Supporting Information for

Discovery of Clonixeril as a Sub-Femtomolar Modulator of the Human STING Receptor

Robert P. Sparks[1,2,3†], William Lawless[1,2,4†], Anna Kharitonova[1,2,4†], Rainer Metcalf[1†], Jamie Nunziata[1], Grace A. Binder[1], Sauradip Chaudhuri[5], Christine S.R. Gambino[1], Michelle Wilde[1], Linette S. Harding[1], Jaret J. Crews[1], Mansi Gopu[1], Emilia Dalamangas[1], Sarah Lawless[1], Mark Eschenfelder[1], Robert M. Green[5], Elizabeth X. Nompleggi[3,7], Timothy Tran[6], Kathy Yang[6], Donna V. Trask[1], Paul R. Thompson[5], Rekha Patel[2,4], Niketa A. Patel[2,4], Wesley H. Brooks[1], W. Guy Bradley[8], Mildred E. Acevedo-Duncan[1], Alan C. Mullen[3], James W. Leahy[1,4,9], Kenyon G. Daniel[1,10], Wayne C. Guida[1,6,9*]

Affiliations:

[1] Department of Chemistry; University of South Florida, Tampa, FL, USA.
[2] Research Service; James A. Haley Veterans Hospital, Tampa, FL, USA.
[3] Division of Gastroenterology, Department of Medicine; University of Massachusetts Chan Medical School, Worcester, Massachusetts, USA.
[4] Department of Molecular Medicine, Morsani College of Medicine; University of South Florida, Tampa, FL, USA.
[5] Biochemistry and Molecular Biotechnology Department; University of Massachusetts Chan Medical School, Worcester, Massachusetts, USA.
[6] H. Lee Moffitt Cancer Center, Research Institute at the University of South Florida; Tampa, FL, USA.
[7] College of the Holy Cross, *Worcester, MA, USA.*
[8] Tampa Bay Research Institute, St. Petersburg, Florida, USA
[9] Florida Center for Drug Discovery and Innovation, University of South Florida, Tampa, FL, USA
[10] Department of Molecular Biosciences, University of South Florida, Tampa, FL, USA.

* Corresponding Author: Dr. Wayne C. Guida, Department of Chemistry, University of South Florida, CHE 205, 4202 E. Fowler Avenue, Tampa, FL 33620, USA.

Table of Contents

Supplementary Text

MD Simulations in Support of Computational Model Construction

We employed molecular dynamics (MD) simulations to better understand how STING interacts with endogenous ligands and other potential binding partners. The distance between the α-carbons of both H185 residues at the end of the α2 helices in dimeric hSTING^{WT} CTD was used as a metric for STING activation. Crystal structures of known agonists showed alpha carbon distances in the range of 34 to 38 Å (PDB: 4EMU) for holo structures, whereas apo crystal structures had alpha carbon distances in the range of 47 to 56 Å (PDB: 4KSY, **Table S2**). Initial binding of ligands to hSTING^{WT} CTD near residues Q266 and T267 stabilizes the disordered "lid" region towards β sheet formation, bringing the α2 helices closer together. This prompted generation of two separate docking models (**Figure 1C**) to screen for (a) agonists, compounds that have greater affinity for the holo (2',3'-cGAMP bound structure), and thus stabilize the ordered lid, and (b) antagonists, compounds biasing a more disordered lid conformation.

Our statistical models were compiled based on deviation from known values and internal variance to adjust for docking and simulation error (**Table S2**). ITC, SPR, and consensus docking energetics for the hSTING wild type (hSTING^{WT}) native ligands 2'3'-cGAMP and c-di-GMP (**Table S2**) are in close agreement, supporting the validity of our MD equilibrated hSTING^{WT} binding models. Due to the dominance of the WT allele in human populations, the MD equilibrated hSTING^{WT} antagonist (PDB: 4F5Y) and hSTING^{WT} CTD agonist (PDB 4KSY) conformations were taken as the two specific docking models for subsequent STING molecular modeling.

Site-Restriction Virtual Screening for Identification of Possible Dimer Complexes

Current docking programs are restricted to docking and evaluating a single molecule at a time. Due to this, docking algorithms are unable to effectively predict ligands which bind as dimers, such as the binding of DMXAA to mouse STING. To overcome this limitation, we developed a simple docking method that can be used in conjunction with standard virtual screening protocols to assist in identifying potential small molecule dimer-protein complexes. Initially while utilizing the entire protein dimer structure, the ligand is restricted to a monomeric half of the binding site (**Figure S2A**). This procedure, as opposed to an alternate docking protocol involving the protein monomer alone, allows for site electrostatics that are consistent between the whole site and the restricted portion. Then, following the typical virtual screening protocol, the whole site (**Figure S2B**) is employed for ligand docking. To avoid oversimplification of the ligand binding geometry and to test assumptions of ligand and half-site interaction, the next step is to implement an RMSD comparison of the ligand poses for the whole and half site docking runs. If the RMSD between the whole and half site poses is less than the commonly accepted 2 Å cutoff, then the docked ligand evidently prefers a specific region in the binding site and should allow for another stoichiometric equivalent of the molecule to bind into the surplus volume. After review of the initial ligand poses, updated docking grids are generated with the original docked compound and the unoccupied region is subsequently screened with a duplicate ligand (**Figure S2C**). The dimer composite structure could then potentially be linked through a zero-ordered bond connecting the two most proximal atoms. For GLIDE, this type of bond only has an enforced distance constraint, angle and dihedral terms are zero, and do not interfere with the molecular force field. Docking the linked dimer (LD) back into the respective protein conformer will allow the docking algorithm to properly calculate estimated free energies of binding for the LD-protein complex.

Differential Scanning Fluorimetry – Thermal Shift Experiment

The change in melting point of hSTING^{WT} CTD (**Figure S1)** was observed in 3 scenarios: 1) bound to the endogenous ligand, 2',3'-cGAMP, 2) unbound and 3) bound to ligands chosen by the virtual screening process for their potential to stabilize the active form of the STING molecule by binding to it. A TSA measures a protein's melting temperature (Tm), at which the protein is 50% denatured. The assay quantifies protein denaturation by measuring the increase in fluorescence of a dye that binds to hydrophobic residues exposed by unfolding of the protein.

Clonixeril Demonstrates Limited Hydrolysis under Digestive Conditions

To determine clonixeril's hydrolytic stability and evaluate its potential as an oral drug, an aqueous solution was concentrated for analysis at 20 µM. The sample was analyzed by HPLC using an isocratic gradient of water and methanol and resulted in spectra demonstrating two distinct peaks. The UV spectra of these peaks were compared by diode array and found to be identical with maximum absorbance at 280nm and 343nm. LC/MS demonstrated that the molecular weight of the minor first peak matched the molecular weight of clonixin (M+H)+ and the second major peak matched the molecular weight of clonixeril (M+H)+. Data was generated by measuring the ratio between the two peaks. Hydrolysis of clonixeril to clonixin was measured by HPLC over seven days using a 20 µM aqueous solution. Initial hydrolysis was found to show 3.2% clonixin and 96.8% clonixeril (**Figure S4B**). Most of the hydrolysis occurred within the first two days at an average rate of 0.13% per hour, and then slowed down to an average rate of 0.07% per hour by day seven (**Figure S4B**). The rate decrease correlated with an observable decrease in solution pH as a product of hydrolysis. Further samples solubilized in pH 2.00 phosphoric acid and pH 1.99 hydrochloric acid confirmed that the rate decreases to an average of 0.014% per hour over a seven-day period. Samples solubilized under basic conditions such as 5% sodium bicarbonate resulted in an increase in initial hydrolysis to 11.8% clonixin and 88.2% clonixeril.

Clonixeril affects pIRF3 production only through the STING pathway

Because pIRF3 can be produced from TBK1 via pathways independent of STING (i.e., TLR7 and MDA5/RIG-I), we tested clonixeril in a STING knockout THP-1 Luciferase assay. The assay method was identical to the one reported in the main text hSTING^{WT}. As is shown in **Figure S4D**, we demonstrate that clonixeril is affecting pIRF3 production only through the STING pathway.

Supplemental Methods

Synthesis of Clonixeril and its Enantiomers

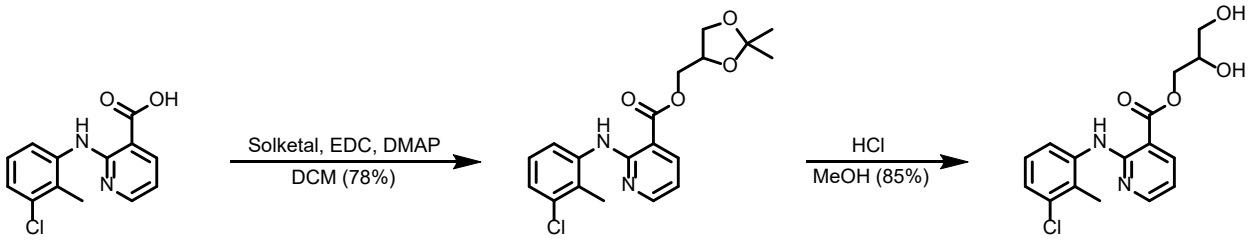

A solution of clonixin (544.3 mg, 2.072 mmol) in dichloromethane (10 mL) was cooled to 0 °C in a round bottomed flask with stirring. Solketal (1.29 mL, 10.4 mmol), EDC (795.1 mg, 4.148 mmol) and DMAP (13 mg, catalytic) were added, and the reaction was stirred at 0 °C for 1 h before warming to room temperature overnight. The reaction was quenched with water (10 mL) then extracted with DCM and the combined organic layers washed with saturated sodium bicarbonate and concentrated on a rotary evaporator to give a gummy residue (609 mg, 78%) that was used without further purification.

A solution of the ketal protected clonixeril obtained above (609 mg, 1.62 mmol) was dissolved in methanol (10 mL) and cooled to 0 °C in a round bottomed flask. A few drops of a solution of 3M HCl in methanol was added, and the reaction was allowed to warm to room temperature overnight. The solution was then concentrated without heat on a rotary evaporator to give a yellow oil that was purified by flash column chromatography (DCM/MeOH 19:1) to give clonixeril (463 mg, 85%) as a colorless oil. ^{1}H NMR (600 MHz, $CDCl_3$) δ 9.75 - 9.83 (m, 1 H), 8.25 - 8.30 (m, 1 H), 8.16 - 8.23 (m, 1 H), 7.73 - 7.78 (m, 1 H), 7.05 - 7.14 (m, 2H), 6.62 - 6.69 (m, 1 H), 4.30 - 4.40 (m, 2 H), 3.97 - 4.04 (m, 1 H), 3.69 - 3.76 (m, 1 H), 3.57 - 3.64 (m, 1 H), 2.31 (s, 3 H) ppm. ^{13}C NMR (151 MHz, CD_3OD) δ 169.3, 156.4, 151.4, 141.2, 138.7, 134.4, 129.0, 126.5, 124.8, 122.2, 113.3, 108.5, 13.6 ppm.

Synthesis of (R)-Clonixeril

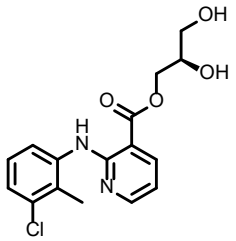

(R)-clonixeril was synthesized using the procedure outlined above for racemic clonixeril, but with commercially available (R)-solketal (obtained from Aaron Chemical) used in place of racemic solketal. (R)-clonixeril had identical analytical data to that obtained above. (S)-clonixeril likewise was prepared using (S)-solketal.

Synthesis of Mefenamic Acid Glycerol Ester

Mefenamic acid glycerol ester was prepared using the procedure described above for clonixeril with the exception of mefenamic acid being employed as a starting material rather than clonixin. Yield 85.0%. ^{1}H NMR (600 MHz, CHLOROFORM-d) δ 9.02 - 9.13 (m, 1 H), 7.82 - 7.91 (m, 1 H), 7.14 - 7.18 (m, 1 H), 7.04 - 7.08 (m, 1 H), 7.00 - 7.04 (m, 1 H), 6.92 - 6.97 (m, 1 H), 6.63 - 6.67 (m, 1 H), 6.55 - 6.59 (m, 1 H), 4.29 - 4.37 (m, 2 H), 3.98 - 4.04 (m, 1 H), 3.69 - 3.74 (m, 1 H), 3.61 - 3.65 (m, 1 H), 2.75 - 3.16 (m, 1 H), 2.35 - 2.70 (m, 1 H), 2.24 (s, 3 H), 2.08 (s, 3 H) ppm. 13C NMR (151 MHz, CHLOROFORM-*d*) δ ppm 168.9, 149.8, 138.5, 138.3, 134.6, 132.6, 131.5, 127.0, 126.0, 123.3, 116.1, 113.8, 110.1, 70.5, 65.3, 63.5, 20.6, 14.0 ppm.

Differential Scanning Fluorimetry (Thermal Shift)

QuantStudio and Protein Thermal Shift Software were used to analyze 2 μM CTD STING protein in 25 μM TBS at pH 8, 2% DMSO and SyproOrange. 57 compounds including CXL were screened at 200 μM to determine melting temperature as compared to controls which were CTD STING protein without 2'3'-cGAMP and CTD STING protein with 200 μM 2'3'-cGAMP as a direct comparison. The T-ramp range was between 25-99 °C within 1 hour.

Solubilization and HPLC Mass Spectrometry of CXL and CXN

A bathtub sonicator was used at room temperature to aid solubilization of CXL. Care was used to avoid heating the solution and causing unwanted hydrolyzation through the addition of vibrational energy supplied from a sonication probe. An isocratic gradient program of mobile phase A (100% water) and mobile phase B (100% methanol) was established on a Shimadzu liquid chromatography system, and the column was initially brought to equilibrium at 10% B. An isocratic gradient program was performed, whereas mobile phase B remained at 10% for the first five minutes and then 10% to 80% gradient from 5 minutes to 35 minutes. A sample was created at 200uM using 100% methanol and 500μL was shot onto Agilent 1260 Preparative HPLC-DAD-MS SQ 6120. Retention times for both peaks were relatively similar. The two peaks were collected, dried using nitrogen, solubilized in acetonitrile, and run on the Agilent LC-MS QTOF 6540.

Phospho-IRF3 Assay

HEK293T cells transfected with hSTING^{WT} cells were seeded in a 6-well plate in DMEM (supplemented with 10% heat-inactivated fetal bovine serum, 1X Corning Penicillin-Streptomycin solution and 0.01mg/mL Blasticidin). Upon reaching ~80% confluence, cells were pretreated with varying concentrations of CXL in FBS-free DMEM for 2 hours. This was followed by treatment with diABZI3 (100nM) for 1 hour. The cells were scraped, harvested by centrifugation at 1000 x g for 3 mins. The resulting pellet is resuspended in 1X PBS with 1X Halt protease & phosphatase inhibitor and 1% NP-40. Cell lysis was performed by probe sonication. The cell lysate is further denatured in 1X SDS loading buffer by boiling for 10 mins and separated by SDS-PAGE (4-20% gel). The separated proteins were electrically transferred to a PVDF membranes separately, which was probed with primary (α-pIRF3, α-IRF3 & α-STING) and secondary (goat anti-rabbit IR dye 680 & goat anti-mouse IR dye 800CW) antibodies. The blots were visualized using a LICOR Image Analyzer. All the experiments were performed at least in duplicate.

Alternative protocol for STING THP1 Competition Reporter Assay with 2',3'-cGAMP as the Activator

In order to permeabilize relatively impermeable CXL analogs, we developed a digitonin-based assay to be used in conjunction with our STING THP1 competition assay. The protocol is given here.

Reporter Cells

THP-1 Dual KI hSTING^{WT} R232 cells (cat no. thpd-nfis) were obtained from Invivogen (San Diego, CA) and processed as per the manufacturer's instructions. The cells were cultured at 37C in 5% CO2 in complete RPMI media (RPMI 1640 GlutaMAX I supplemented with sodium bicarbonate (2.0 g/L), D-glucose (2 g/L), 10% fetal bovine serum, penicillin (100U/mL), streptomycin (100 μg/mL) and Normocin (100 μg/mL). The cultures were maintained at cell densities between 5 x 10^5 and 2 x 10^6/mL.

Digitonin facilitated STING THP1 Cell assay

Prepared the treatment solutions in 5 mL polystyrene snap cap tubes (labeled A-G). Tube A (negative control) contained 1.5 mL digitonin buffer (DB; 50 mM HEPES pH 7.0, 100 mM KCl, 3 mM $MgCl_2$, 0.1 mM DTT, 85 mM sucrose, and 0.2% BSA) only. Ten mL of DB and 1.25 ug/mL digitonin (stock is 10 mg/mL in H2O) were added to a 15 mL conical polypropylene tube, mixed well, and then 1.5 mL of this solution was aliquoted into tubes B-G. Starting with a Clonixeril concentration of 1 µM in Tube C, 1000-fold serial dilutions were generated (1nM, 1pM, 1fM, and 1 aM). Transferred 5 x 10^5 of freshly harvested THP-1 Dual KI hSTING R232 cells into seven 5 mL snap cap polystyrene tubes labeled 1-7. Pelleted the cells using a Clay Adams Sero-Fuge II centrifuge at 1000 x g for 2 minutes. The media was carefully removed by aspiration. Each pellet was suspended in 1 mL of the treatment solutions (A-G, respectively) vortexed to ensure mixing. The cells were incubated at 37°C for 10 min. Then, as quickly as possible, 10 µL of a 1 mM stock solution of 2'3' cGAMP was added to each tube and vortexed to mix. The cells were incubated at 37°C for 10 min. At the end of the 10 min treatment, 2 mL of complete phenol red free RPMI (10% FCS, 1x penicillin/streptomycin) was immediately added to all tubes and mixed well. The cells were centrifuged for 2 min at 1000 x g. The supernatant from each tube was removed, the cells suspended in 500 µL of fresh phenol-red free complete RPMI media and incubated at 37°C for 4 to 24 h (preferably 6 h).

Detection of IRF3 gene activation

After the 6 or 24 h incubation, the cells in each tube were vortexed and then 20 µL of the cells were transferred into quadruplicate wells of a solid white plate. The detection of luciferase generated by the THP-1 Dual KI hSTING R232 cells was performed using Invivogen's QUANTI-Luc 4 Lucia/Gaussia solutions and the associated "glow" protocol. Using a multichannel pipet, 50 µl of the QUANTI-Luc™ 4 Lucia/Gaussia "Glow" solution (with added stabilizer) was added to each well and gently mixed. The plate was immediately placed in Modulus Microplate reader and the relative light units (RLU) were measured using an integration time of 0.5 sec.

Supplementary Tables and Figures

Table S1. Summary of K_d values for some biophysical data

CPD	Technique	K_d
Cyclic-DiG	SPR - Steady State	4.8 μM
2',3'-cGAMP	SPR - Steady State	3.56 nM
Clonixeril	SPR - Steady State	430 nM
Clonixin	SPR - Steady State	637 nM
Cyclic-DiG	ITC	2.17 μM
2',3'-cGAMP	Thermophoresis + 50 nM 2',3'-cGAMP	4.00 nM
Clonixin	Thermophoresis + 50 nM 2',3'-cGAMP	~500 nM
MFA	Thermophoresis + 50 nM 2',3'-cGAMP	No Shift

Table S2. Computer Model Comparisons of Literature and Experimental Values

Structure	Compound	H185 Distance (Angstroms)	H185 Post-MD Distance (Angstroms)	Model K_D (nM)	SPR K_D (nM)	ITC K_D (nM)	Cell EC_{50} (nM)
hSTING^{WT}	c-2'3'-GAMP	35.0[a]	37.8	2.4	1.4	3.8[a]	42 (IFNβ mRNA)[a]
	c-2'2'-GAMP	-	43.1	256	-	287[a]	16 (IFNβ mRNA)[a]
	c-di-GMP	53.0[c]	56.5	6377	4776	1210[a]	538 (IFNβ mRNA)[a]
hSTING^{REF}	c-2'3'-GAMP	34.7[b]	39.3	784	-	5300[b]	1200 ELISA[b]
	c-2'2'-GAMP	38.4[b]	41.9	236	-	2500[b]	3400 ELISA[b]
	c-di-GMP	52.6[d]	54.1	1300	-	4600[c]	ND (IFNβ Luc)[c]
						4420[d]	ND (IFNβ Luc)[d]

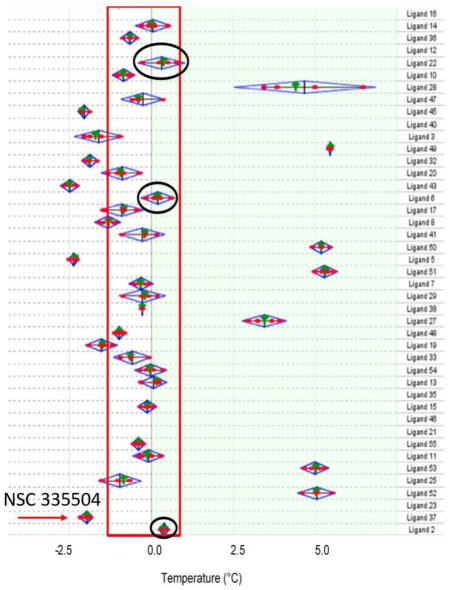

Figure S1. Differential Scanning Fluorimetry (Thermal Shift) for Binders of STING.
Compounds selected (57) from computational virtual screening for analysis at 200 μM in the thermal shift assay are shown here as green dots with blue diamond indicating the temperature range of denaturation. The red box indicates the hSTING CTD control with 200 μM 2',3'-cGAMP at 5.47, 5.19, 5.29, 5.00 5.05 ºC respectively. Black ovals are compounds with significant ΔTm above the hSTING CTD. Clonixeril (NSC 335504) is ligand 37.

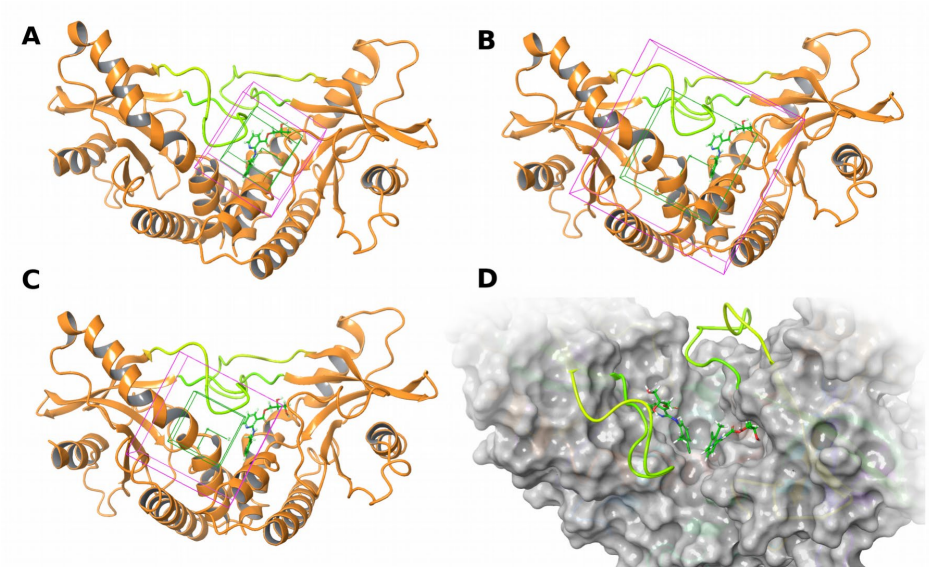

Figure S2. Structures of hSTING (CTD) with Clonixeril bound. Green boxes indicate ligand centroid positional constraint and purple boxes represent all ligand atom positional constraint. Lid region demarcated with yellow-green ribbons. (A) Site-restriction docking method for identifying potential dimeric ligand complexes. Initial docking to monomer unit of binding site is performed with half of the site excluded. (B) Secondary re-docking of ligand is performed with no restrictions. (C) If ligand maintains its pose in both docking simulations, a second copy of the ligand is re-docked to a new grid with the original ligand held in place. The re-docked copy can then link to the initial pose with a zero-order bond, connecting the most proximal atoms, and re-docked once more (D) Antagonist model with two CXL molecules bound shown (molecular surface shown for clarity).

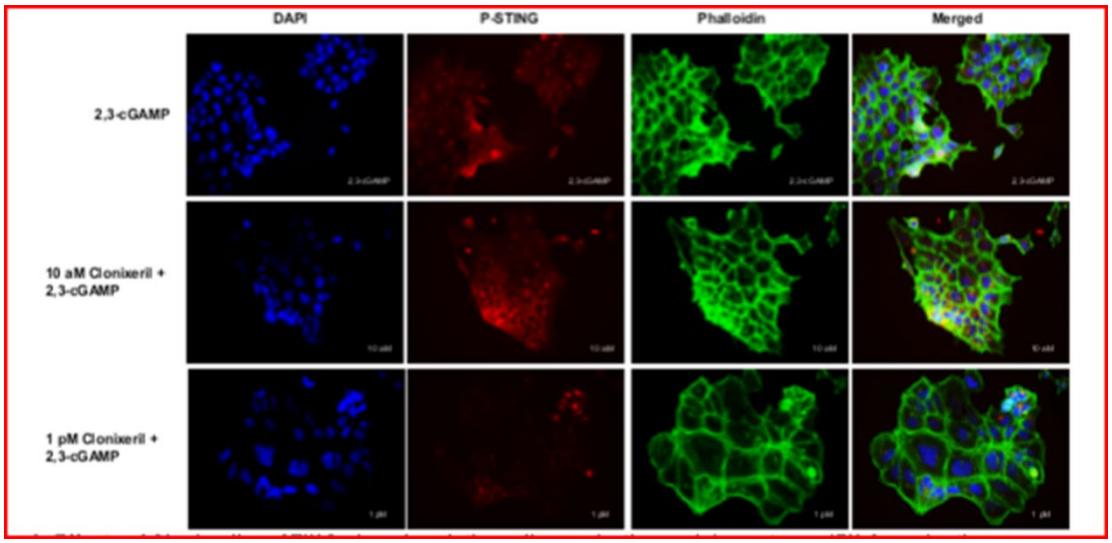

Figure S3. Immunocytochemistry of HEK293 cells showing pSTING. HEK293 cells were treated with 10 aM or 1 pM clonixeril in the presence of 2 µM 2',3'-cGAMP. Cells were incubated with pSTING rabbit primary antibody followed by Alexa 594 anti-rabbit secondary antibody. Cells were stained using phalloidin conjugated to FITC (488) in a solution containing 4',6'-diamidino-2-phenylindole (DAPI). Images were taken using a Fluorescent Microscope.

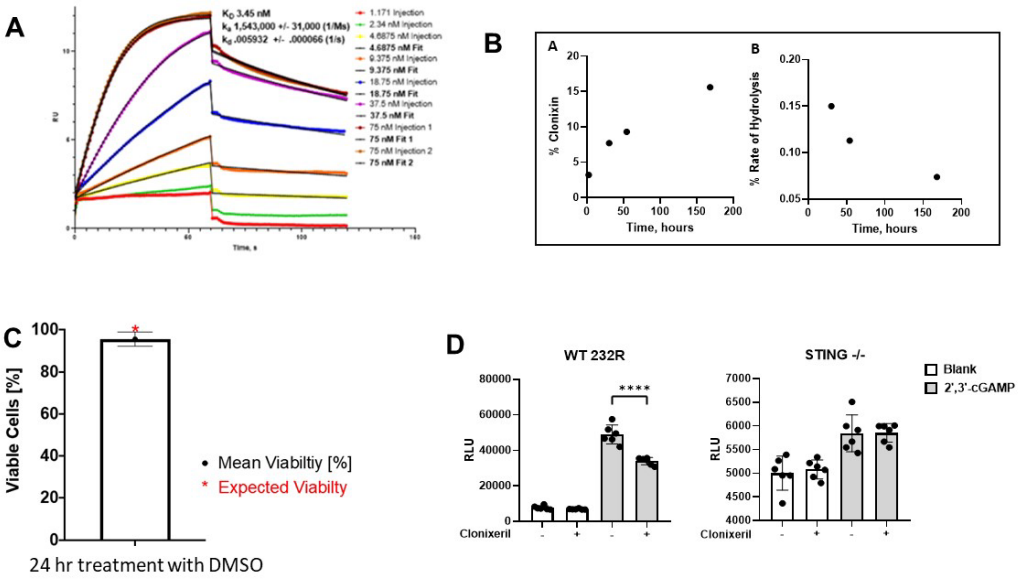

Figure S4. SPR, Clonixeril Stability, Cell Viability, and THP1 STING Knockout Data. (A) SPR analysis for 2',3'-cGAMP interaction using hSTING CTD. (B) Hydrolysis of clonixeril in aqueous solution over seven days with change in rate of hydrolysis plotted over seven days. (C)THP-1 cell viability. DMSO concentration 0.1%. (D) Quantification of luciferase assay performed using WT-THP1 and THP1 STING knockout cells in the presence and absence of clonixeril and/or 2',3'-cGAMP. White indicates absence of 2',3'-cGAMP, gray indicates 2',3'-cGAMP is present. Plus (+) indicates addition of clonixeril, minus (-) indicates clonixeril's absence. Gray indicates 2',3'-cGAMP is present. Note the difference in RLU values in the STING -/- experiment.

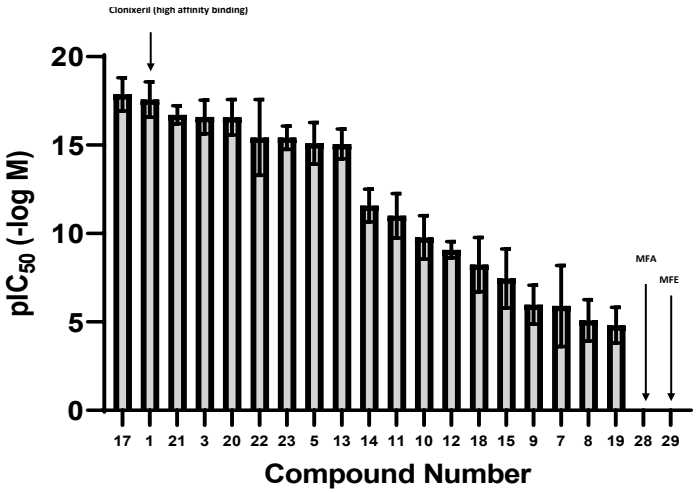

Figure S5. SAR for Clonixeril and Analogs. Summary for 21 selected compounds from an analog library of over 40 compounds screened by MST. EC50 values are shown on a log scale. Compound 1 is CXL. Error bars are standard deviations.

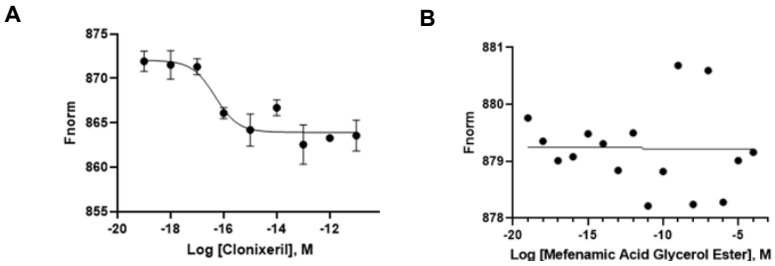

Figure S6. MST for Clonixin and Mefenamic Acid Glycerol Ester. (A) MST analysis for clonixin; titration shown is from 100 zM to 10 μM; N=3. (B**)** MST analysis for mefenamic acid glycerol ester; titration shown is from 100 zM to 10 μM; N=3.

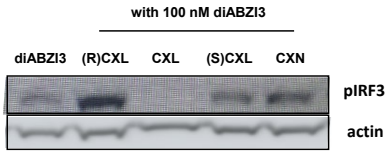

Figure S7. Western Blot for HEK293S cells treated with Clonixeril and its enantiomers. Western blot of HEK293S cells treated with 100 fM clonixeril, R-clonixeril, S-clonixeril, and clonixin in the presence of 100 nM diABZI3.

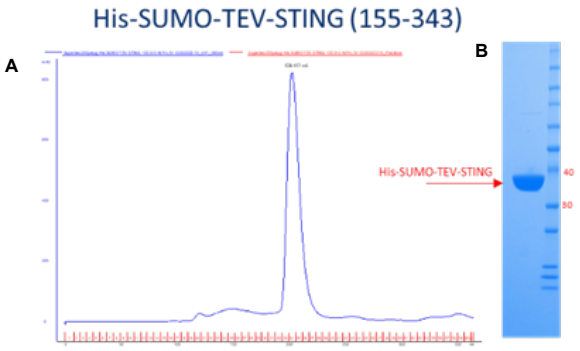

Figure S8. Purity of His-SUMO-TEV-STING. (A) HPLC trace (B) SDS PAGE. Lane 1: Purified His-SUMO-TEV-hSTING CTD; Lane 2 MW marker.